NTIA Report TR-04-407

Relative Propagation Impairments Between 430 MHz and 5750 MHz for Mobile Communication Systems in Urban Environments

Peter Papazian
Michael Cotton

U.S. DEPARTMENT OF COMMERCE
Donald L. Evans, Secretary

Michael D. Gallagher, Acting Assistant Secretary
for Communications and Information

December 2003

Disclaimer

Certain commercial equipment, instruments, or materials are identified in this report to specify the technical aspects of the reported results. In no case does such identification imply recommendation or endorsement by the National Telecommunications and Information Administration, nor does it imply that the material or equipment identified is necessarily the best available for the purpose.

CONTENTS

Page

FIGURES

Page

TABLES

Page

EXECUTIVE SUMMARY

This report describes mobile radiowave propagation measurements made in the downtown area of Denver, Colorado. The measurements were made to determine the relative nature of propagation impairments over a range of frequencies proposed for new communication services. In some cases these proposals would require moving existing commercial services or military communication systems to make way for new broadband mobile communication services. The argument for moving existing fixed services is that lower frequencies that suffer fewer propagation impairments are better suited to mobile applications. This work measures these propagation impairments so these questions can be addressed quantitatively.

Broadband mobile impulse response data were collected at 430 MHz, 1360 MHz, 2250 MHz and 5750 MHz. These frequencies begin at the lower end of the UHF TV band at 430 MHz, proceed to the lower end of the SHF band at 1350 MHz, then jump to 2250 MHz, which is near spectrum being sought for 3G mobile services, but presently occupied by US military radars, and then jump to 5750 MHz, which is an ISM band being considered for broadband wireless access and possibly for 3G wireless applications instead of 2 GHz frequency bands.

Consequently, the relative propagation impairments between 2 GHz and 5.75 GHz are of particular interest for 3G services. The lower frequency range (430 and 1350 MHz) serves as a reference concerning the frequency dependence of propagation parameters. This large frequency range helps establish a trend for the propagation parameters and is useful for comparison with other measurements.

Propagation parameters are highly dependent upon the environment and system configuration such as antenna height and transmitter receiver separation. These were chosen to match the urban mobile cellular environment. But even in an urban cellular environment these parameters can vary greatly. So to measure the relative effects versus frequency, all frequencies were transmitted simultaneously and the data collected simultaneously at the same locations. To compensate for environmental effects, three different urban routes were chosen and statistics from each route were compared. One route was an urban boulevard with line-of-sight paths (S1R1), another was an urban high-rise, urban low-rise, line-of-sight area (S1R2), and the third was an urban high-rise environment (S2R2).

The measurement system utilized a 4-channel pseudonoise code transmitter chipping at 10 MB/s. This allowed measurement of the radio channel impulse response at 4 carrier frequencies with a resolution of 100 ns and a bandwidth of 20 MHz. The data were digitized at IF which allows post processing to determine all radio propagation metrics. The metrics chosen for study were the basic transmission loss (L_b) and delay spread S. To quantify L_b, average slope and σ about the local mean were determined. These metrics allow coverage calculations and link budget analysis at specified availability levels using a simple radio propagation model. The second metric S is used to quantify multipath and signal dispersion. These propagation impairments can cause intersymbol interference and

limit the transmission bit rate, bandwidth, and performance of digital communication systems.

Figure ES1 shows the three drive routes and the transmitter site in downtown Denver, CO. Bursts of impulse response data were collected simultaneously at 4 measurement frequencies at positions marked on the street map. An example of L_b measurements at 430 MHz is shown in Figure ES2. Similar maps for L_b and S at all measurement frequencies are contained in the main body of the report and the appendix.

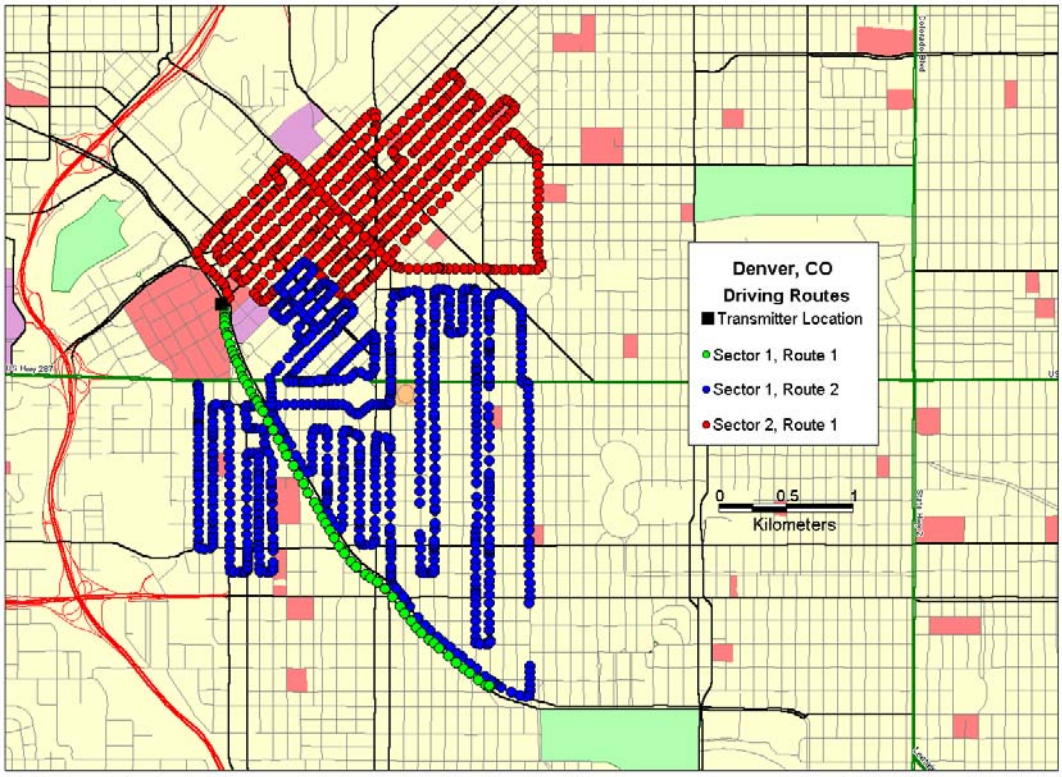

Figure ES1. Drive route map for radiowave propagation survey in downtown Denver, CO.

To quantify the relative nature of L_b versus frequency, the data were assembled by route and plotted versus log distance from the transmitter. In this format a simple propagation model for mobile communications can be used. This model characterizes the transmission loss using the average slope and the distribution of L_b around its local mean value. It has been found that if fast fading (Rayleigh fading) is averaged out, the slow fading is lognormally distributed with a standard deviation σ. Figure ES3 shows such an analysis for sector 1 route 1 (Speer Blvd. shown in green on Figure ES1). On ES3 three distinct regions can be seen. These regions are analyzed relative to the free space loss curve (red) and the average slope (green line) of the measured points determined using a least squares fitting method. Close in to the transmitter, data points in red indicate propagation paths that were shadowed by the transmitter building or are in the side lobes of the

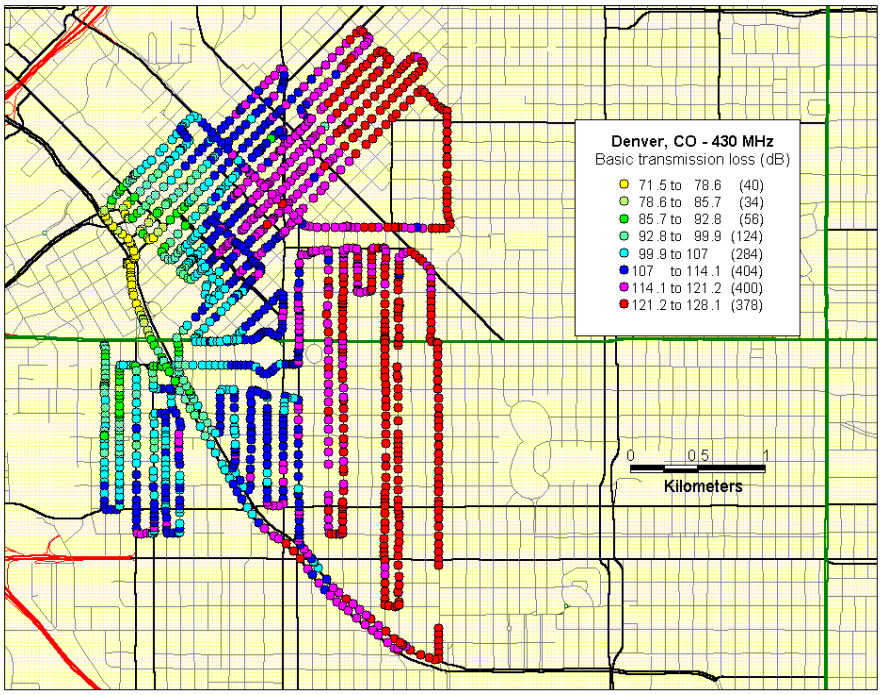

Figure ES2. Basic transmission loss (L_b) at 430 MHz all routes for downtown Denver, CO.

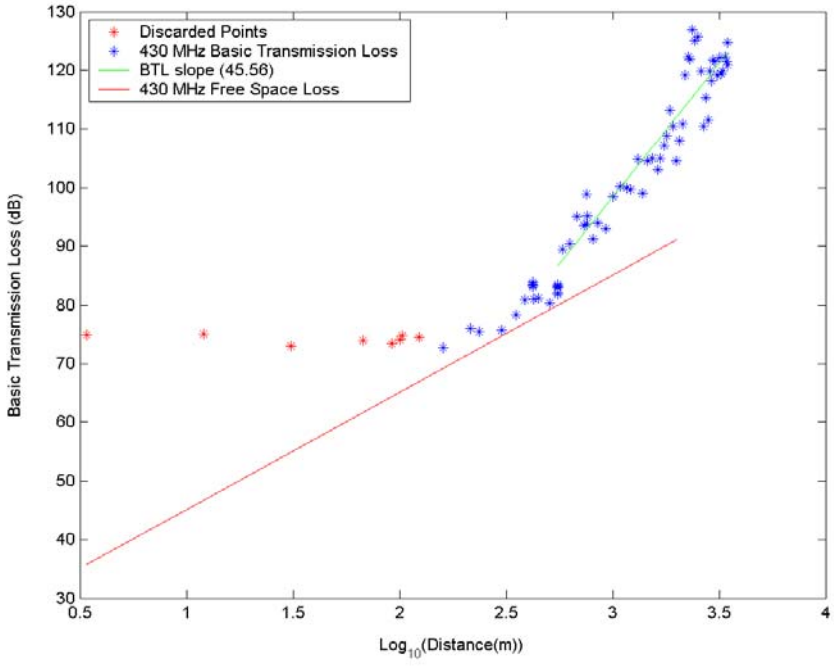

Figure ES3. Basic transmission loss versus distance, sector 1 route 1, at 430 MHz.

transmit antennas. At log distances between 2 and 3 (100 to 1000 m), the data points are closely aligned with the free space loss curve (red). This indicates a line-of-sight propagation region. Then the slope increase (green versus red lines) indicates signal shadowing and diffraction. It is this area where the average path loss slope ($\Delta L_b/\Delta r$) is used to quantify the relative propagation impairments due to the environment. Similar analysis including the σ for lognormal fading about the green trend line is included in the main body and appendix of the report. Table ES1 is a summary of the path loss slope for the different drive routes. We see on average the slope increased from 43 to 54 dB/decade between 430 and 5750 MHz. Between 2250 MHz and 5750 MHz the slope increase was between 1 and 5 dB, and 3.5 dB on average.

Table ES1. L_b Slopes for Three Routes in the Downtown Area of Denver, CO

	$\Delta L_b / \Delta r$ (dB/decade)			
Route	430 MHz	1350 MHz	2260 MHz	5750 MHz
S1R1	45.1	57.7	54.3	59.1
S1R2/urban	40.4	46.1	48.0	49.1
S2R1	42.3	48.8	47.9	52.7
Average	42.6	50.8	50.1	53.6

These results are also displayed graphically in Figure ES4. Here the data is plotted versus log frequency and we see that the path loss slope trend versus frequency shows a linear increase of about 11 dB/decade.

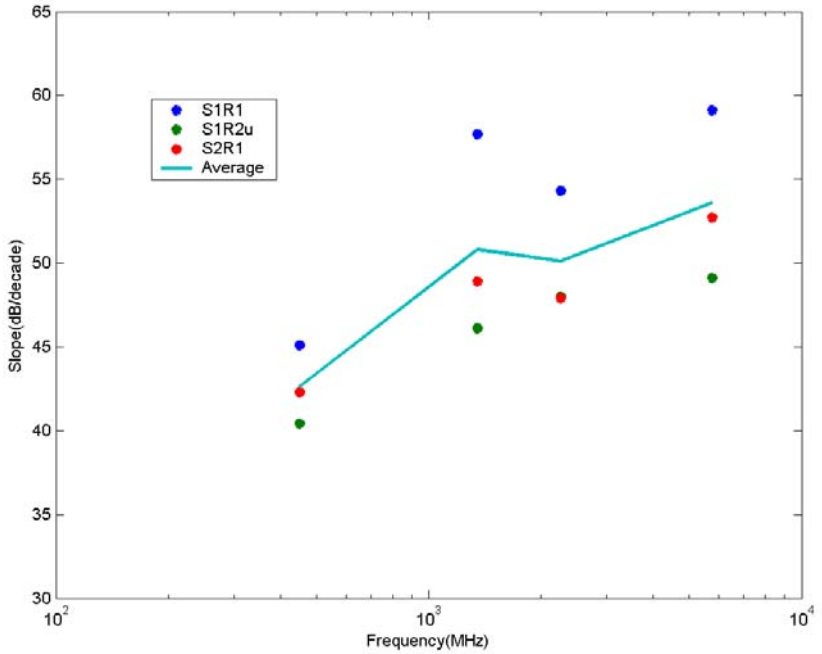

Figure ES4. L_b slope versus frequency for three urban drive routes in Denver, CO.

The σ for the distribution of path loss around the best-fit line is given in Table ES2. These values are consistent with measurements made in urban areas in the PCS bands. By

using the path loss slope and σ, link budget calculations can be made at different availability levels versus frequency. No clear trend was seen in this data except on the urban high-rise route (S2R1) where the standard deviation (σ) of L_b increased with frequency.

Table ES2. σ for Three Routes in the Downtown Area of Denver, CO

	σ (dB)			
Route	430 MHz	1350 MHz	2260 MHz	5750 MHz
S1R1	4.2	3.4	3.4	4.0
S1R2	6.9	6.5	6.7	*
S2R1	4.7	4.5	5.6	6.8
Average	5.3	4.8	5.2	5.4

The cumulative distribution function (CDF) of S is used to analyze the environmental and frequency dependences of the multipath. Using averaged impulse response data, S was calculated and CDF's were computed for different routes and carrier frequencies. Figure ES5 is an example of the CDF's for S2R1. The exceedance probability at 50% (median) and 10% were compiled and it was found that S decreased at higher frequencies. These results are summarized in Table ES3. For instance the average (over all routes) delay spread exceeded 50% of the time (median) decreased from 0.7 μs at 430 MHz to 0.27 μs at 5750 MHz. Similarly the 10% exceedance level dropped from 1.2 μs to 0.68 μs.

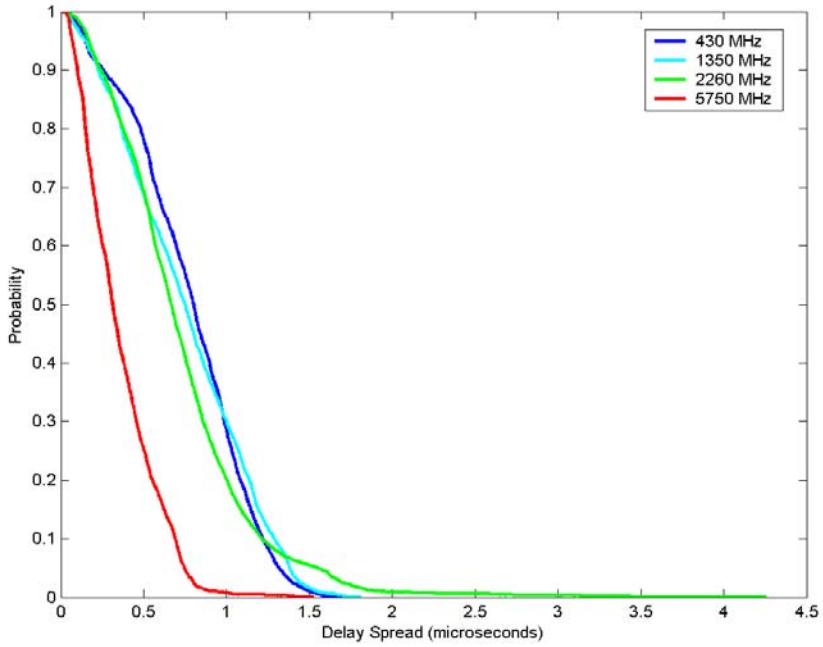

Figure ES5. Cumulative distribution of delay spreads, sector 2 route 1, 430-5750 MHz.

Table ES3. Delay Spread Cumulative Distribution Summary at 50% and 10% Quantiles by Drive Routes with Averages

Ordinate Exceeded	*S (μs) 50%*				*S (μs) 10%*			
Frequency (MHz)	430	1350	2260	5750	430	1350	2260	5750
S1R1	0.3	0.2	0.3	0.1	.95	0.6	0.8	.35
S1R2	0.9	.85	0.8	0.3	1.3	1.4	1.4	1.0
S2R1	0.8	.75	0.7	0.4	1.2	1.3	1.2	0.7
Average	0.7	0.6	0.6	.27	1.2	1.1	1.1	.68

Based on this data several conclusions can be reached concerning the relative propagation impairments between 430 MHz, 1360 MHz, 2250 MHz, and 5750 MHz in urban areas.

1. L_b slope increases linearly versus log frequency at about 11 dB per decade.

2. L_b slope between 2260 and 5750 MHz increases on average by 3.5 dB.

3. Average median *S* decreases by 61% and by 43% at the 10% exceedance quantiles.

These results quantify the additional power requirements needed as carrier frequency increases. The measurements also indicate a decrease in *S* that is beneficial for large bandwidth and higher data rate communication systems.

RELATIVE PROPAGATION IMPAIRMENTS BETWEEN 430 MHZ AND 5750 MHZ FOR MOBILE COMMUNICATION SYSTEMS IN URBAN ENVIRONMENTS

Peter Papazian and Michael Cotton[1]

Radiowave propagation measurements made in an urban area of Denver, Colorado, are described. Wideband, impulse response measurements were made at 4 carrier frequencies from 430 MHz to 5750 MHz. These measurements were made using a mobile measurement van to characterize the mobile communications environment. Basic transmission loss and delay spread are characterized by analysis of the path loss slope and delay spread statistics. By analyzing the results versus carrier frequency the relative propagation impairments for communication systems at 430, 1350, 2260 and 5750 MHz are compared. It was found that the path loss slope increased on average by 11 dB/decade and the delay spread decreased from 33% to 65% over the decade of frequencies measured.

Key words: basic transmission loss; delay spread; impulse response; path loss; radiowave propagation; urban environment.

1. INTRODUCTION

A mobile radiowave propagation survey was conducted in downtown Denver, Colorado, using spread spectrum signals to measure the radio channel impulse response over a 20-MHz bandwidth. The propagation data were collected at 4 carrier frequencies that spanned the decade of frequencies between 430 and 5750 MHz. The purpose of this work was to determine relative propagation impairments for mobile communications over a wide range of frequencies and to create a measurement database to verify the accuracy of existing radio propagation models in an urban environment.

This report is organized as follows. Section 2 is a description of the measurement system. Section 3 describes the survey location, antennas, EIRP, and drive routes. Section 4 describes the data processing. Section 5 presents an analysis of the basic transmission loss and delay statistics. These results include the relative propagation impairments versus frequency. Section 6 gives the conclusions. The data set is archived and can be used for additional modeling and analysis.

[1]The authors are with the Institute for Telecommunication Sciences, National Telecommunications and Information Administration, U.S. Department of Commerce, Boulder, Colorado, 80305.

2. MEASUREMENT SYSTEM

The wideband measurement system [1,2,3] collected impulse response data by transmitting a psuedo noise (PN) code at a rate of 10 Mb/s using BPSK modulation. The received IF signal was digitized, allowing for measurement of the received power and software correlation of the PN signal for the calculation of the radio channel impulse response and other associated propagation metrics. The data were collected simultaneously at all 4 frequencies using precision rubidium time standards at the transmitter and at the receiver, and were stamped with GPS coordinates, heading, and velocity of the receiving van.

3. SURVEY LOCALE, ANTENNAS AND DRIVE ROUTES

The drive routes covered a combination of urban high-rise, urban low-rise and line-of-sight propagation paths in a downtown area of Denver, Colorado. The survey was conducted in the springtime just before the trees leafed out, and during the daytime under average traffic conditions. Four vertically-polarized antennas were used for transmitting radio signals from a rooftop location. The boresight directions of the transmit antennas were adjusted to cover all drive routes by dividing the survey area into two 90° sectors. The 4 omni-directional vertically polarized receiver antennas were mounted over a ground plane on the measurement van.

3.1 Transmitter Site, Antennas and Drive Routes

The transmit antennas were positioned on the SE corner of the University of Colorado Denver North campus building overlooking Speer Boulevard at an elevation of 17 m above the ground. Figure 1 shows the transmit antennas with a view looking to the SE towards sector 1. Figure 2 shows the same antennas but the view is to the east towards the urban high-rise area of sector 2.

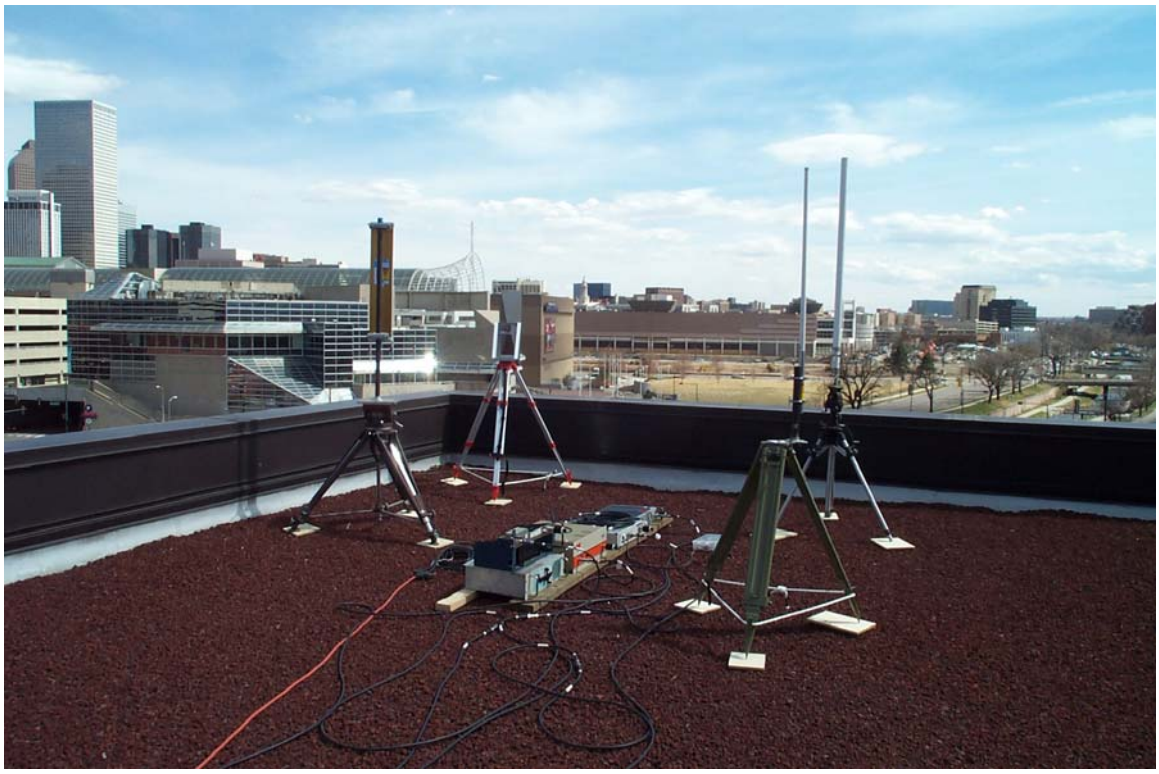

Figure 1. Transmitter site looking SE along Speer Boulevard.

The 2 sectors were surveyed separately by changing the boresight direction of the transmit antennas. The transmit antennas for sector 1 had a boresight direction of S45°E. The drive routes for sector 1 covered Speer Boulevard to the south and both urban low-rise and urban high-rise to the east and west of Speer Boulevard. Figure 3 shows a view of Speer Blvd. Sector 2 covered the northeast survey area and the transmit antennas' boresight was directed N45°E. The drive route for sector 2 covered the urban high-rise areas of downtown Denver. Figure 4 shows a view looking east from the transmitter into sector 2 along an urban canyon formed along Arapahoe Street. Figure 5 is a map showing the drive routes and measurement locations. Sector 1 route 1 is the Speer Blvd. route shown in green. Speer Blvd. is a large boulevard with buildings set back from the drive route. It offers an unobstructed view of the transmitter until it curves eastward. Sector 1 route 2 (blue) has a mixture of low-rise to the west of Speer Blvd. and high-rise and low-rise to the east of Speer Blvd. The downtown high-rise buildings shadow part of this route to the SE. Sector 2, route 1 (red) is an urban high-rise area. These buildings create canyons for radiowave propagation to the east of the transmitter site. The colored circles on the drive route map indicate locations where bursts of 128 impulse response measurements were collected on all 4 channels. These locations are based on the GPS coordinates of the vehicle at the end of the burst. The vehicle velocity and heading are also recorded from the GPS string.

Figure 2. View from the transmitter site looking east towards downtown Denver.

Survey parameters are summarized in Tables 1-4. Table 1 gives the transmitter coordinates and elevation. Tables 2 and 3 list the transmitter and receiver antenna specifications and Table 4 lists transmitter EIRP by frequency.

3.2 Receiver Antennas

Receive antennas were positioned over a conducting ground plane 2.5 m above the street on the roof of the measurement vehicle (Figure 6). These antennas consisted of two monopole antennas and two vertical bicones (See Table 3).

Figure 3. View along Speer Boulevard south from the transmitter site.

Figure 4. View of downtown Denver looking east from the transmitter site.

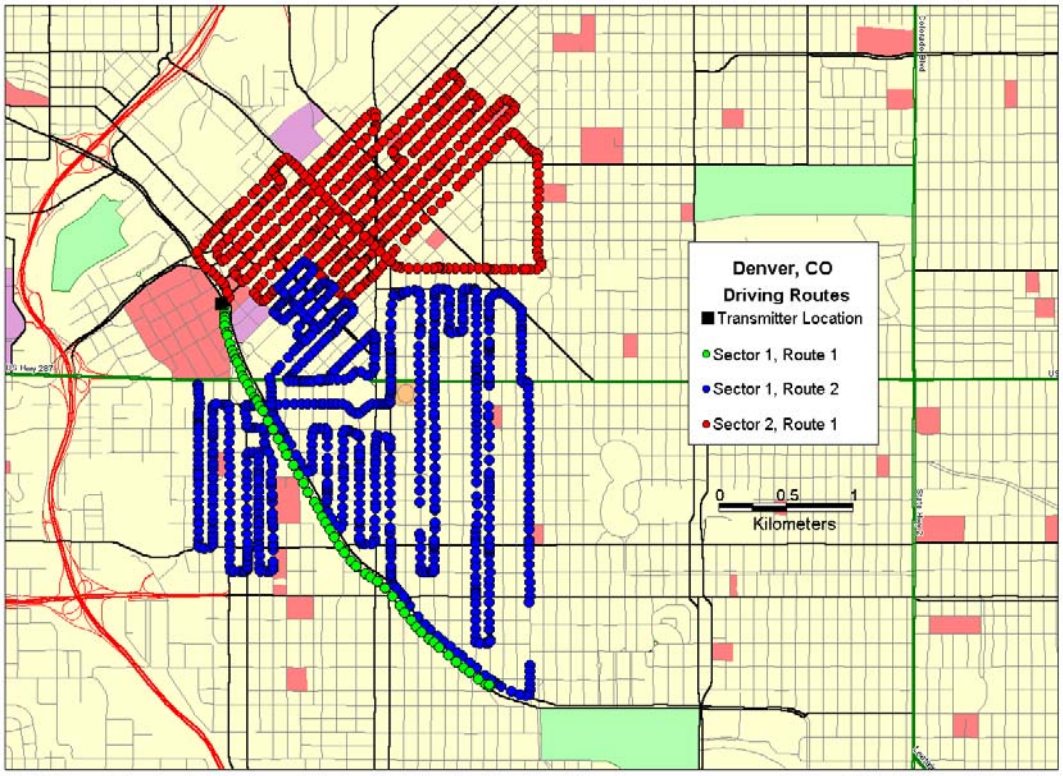

Figure 5. Drive route map for radiowave propagation survey in downtown Denver, CO.

Figure 6. The measurement van, ground plane and receiving antennas.

Table 1. Transmitter Site Coordinates and Antenna Boresight Directions

Sector	Latitude (deg)	Longitude (deg)	Elevation (m)	Boresight
1	39.74521	-105.0013	17	S45°E
2	39.74521	-105.0013	17	N45°E

Table 2. Transmit Antenna Specifications

Antenna	Frequency (MHz)	Vertical BW (deg)	Horizontal BW (deg)	G_t (dBi)	Antenna Type*
Cushcraft FRX-430	430-450	24	Omni	1.7	Stacked Dipole
Dorne&Margolin Q130	1360	11	140	11.3	Stacked Dipole
Decibel DB975H90N-S	2300-2500	9	90	15.2	Stacked Dipole
TECOM 201101	1000-12400	65	100	7.5	Log Periodic

* Vertical Polarization

Table 3. Receive Antenna Specifications

Antenna	Frequency (MHz)	Vertical BW (deg)	Horizontal BW (deg)	G_r (dBi)*	Antenna Type (Vertical Polarization)
Larson	430-440	20	Omni	2	5/8 λ Monopole
¼ Wave	1340-1360	30	Omni	-1.3	¼ λ Monopole
Tecom 201093V	2250-2270	50	Omni	3.9	Biconical
Tecom 201093V	5740-5760	45	Omni	2.0	Biconical

* On the Horizon

Table 4. The Power at Antenna Terminals and EIRP Transmitted versus Frequency

Frequency (MHz)	P_t (dBm) at antenna terminals	G_t (dBi)	EIRP (dBm)
420-440	36.6	1.7	38.3
1340-1360	35.6	11.3	46.9
2250-2270	36.2	15.0	51.2
5740-5760	35.1	7.5	42.6

4. DATA PROCESSING

4.1 Basic Transmission Loss

Data processing algorithms were used to reduce the data to several metrics for analysis. The basic transmission loss (L_b), also called the path loss, is one such metric. It is the transmission loss expected between two ideal, loss-free, isotropic transmitting and receiving antennas. L_b is determined using Equation 1.

$$L_b(dB) = P_t(dB) + G_t(dB) + G_r(dB) - P_r(dB) \tag{1}$$

where:
P_t = *power at transmitter antenna terminals,*
P_r = *power at receiver antenna terminals,*
G_t= *transmit antenna gain above isotropic,*
G_r= *receive antenna gain above isotropic.*

The transmitter power, P_t, is measured using a wideband power meter connected at the end of the transmitter antenna cables. Received power, P_r, is then measured by integrating the receiver's digitized IF signal voltage and subtracting an average calibration constant as in Equation 2.

$$P_r = 10 \times \log_{10}\left(\frac{1}{\tau}\int_o^{\tau} {V_{IF}}^2(t)\,dt\right) - \overline{P_{cal}}(dB) \tag{2}$$

The average calibration constant, $\overline{P_{cal}}$, is determined during the system calibration. In the calibration configuration the transmitter output and receiver input cables are connected using an N type barrel. After measuring the transmitter output, again using a wideband power meter, a series of precision fixed and variable attenuators are used to adjust the transmitter output power at the barrel connector, P_N, between –35 dBm and –105 dBm in 10-dB steps. At each step a burst of data is collected on all receiver channels. After averaging each burst of data, the calibration constant is calculated using Equation 3.

$$P_{cal} = P_N - 10 \times \log_{10}\left(\frac{1}{\tau}\int_o^{\tau} {V_{IF}}^2(t)\,dt\right) \tag{3}$$

The linear range of the receiver is determined and the average calibration constant over this range, $\overline{P_{cal}}$, is used in Equation 2. This calculation is performed for each receiver channel corresponding to the 4 measurement frequencies. In this way the gain of each receiver channel is measured and subtracted from the received power measurements in Equation 2. L_b can now be calculated from the raw data using Equation 1, the antenna gains and transmit powers in Tables 2, 3, and 4.

4.2 Delay Spread

The delay spread (*S)* is a statistical measure of the signal dispersion or multipath. This dispersion is caused by reflections of radiowaves by obstructions between the transmitter and receiver. To calculate *S*, first the digitized IF signal is converted to baseband in software and then correlated with a copy of the transmitted PN sequence. The correlation output is the radio channel impulse response *H(t)*. The power delay profile (PDP) is then calculated by squaring the channel impulse response (Equation 4). The PDP is then averaged over a stationary data burst consisting of 64-128 PDP recordings. The averaging distance is between 10 and 110 λ, depending upon frequency and vehicle speed. This average PDP is called the APDP (Equation 5). *S* is then calculated by computing the second central moment of the APDP using Equations 6 and 7.

$$PDP = \left| H(t_k) \right|^2 \tag{4}$$

$$APDP(t_k) = \frac{1}{N} \sum_{i=1}^{N} PDP_i(t_k) = P(t_k) \tag{5}$$

$$S = \left[\frac{\sum_{k=1}^{N} (t_k - d)^2 P(t_k)}{\sum_{k=1}^{N} P(t_k)} \right]^2 \tag{6}$$

where

$$d = mean\ delay = \frac{\sum_{k=1}^{N} t_k P(t_k)}{\sum_{k=1}^{N} P(t_k)} \quad . \tag{7}$$

5. RESULTS

5.1 Data Overview

Basic transmission loss (L_b) is computed using the digitized IF data, as described in section 4.1. Fast fading is removed from L_b by both integrating the received power, and averaging spatially. First the IF signal is sampled 2044 times at 25 ns intervals. The sample period, 51.1 μs, is equal to the PN word length. After a delay of 3 ms the IF is sampled again until there are 128 independent data sequences. IF data, from each sequence, are used to calculate the received power using Equation 2. The 128 power samples are then averaged to remove the fast fading. The delay spread (S) is calculated using the channel impulse response calculated from the IF data as described in section 4.2. The impulse data are also averaged before the delay spread calculation.

Measurements of L_b for all drive routes and 4 frequencies versus the GPS coordinates of each data burst are shown in Figures 7-10. For an average drive speed of 15 m/s and an impulse-sampling rate of 3 ms, this gives a spatial average every 5.7 m. In wavelengths this corresponds to 108λ, 46λ, 26λ, and 8.5λ for measurement frequencies of 5.75, 2.26, 1.35, and .45 GHz respectively. After averaging, fast fading is removed and only the slow fading caused by terrain and shadowing is left [4,5]. The S data is averaged over the same data bursts with the added constraint that each impulse in the burst has to have a minimum peak to tail ratio of 23 dB. In addition, each burst has to have at least 7 out of 128 impulses that meet these criteria in order to be processed for S. If the data burst meets these criteria, Equations 6 and 7 are used with a 20 dB cutoff to calculate an average S for the burst. Figures B1-B4 (Appendix B) show the average value of S for each burst of data in map view also versus GPS coordinates.

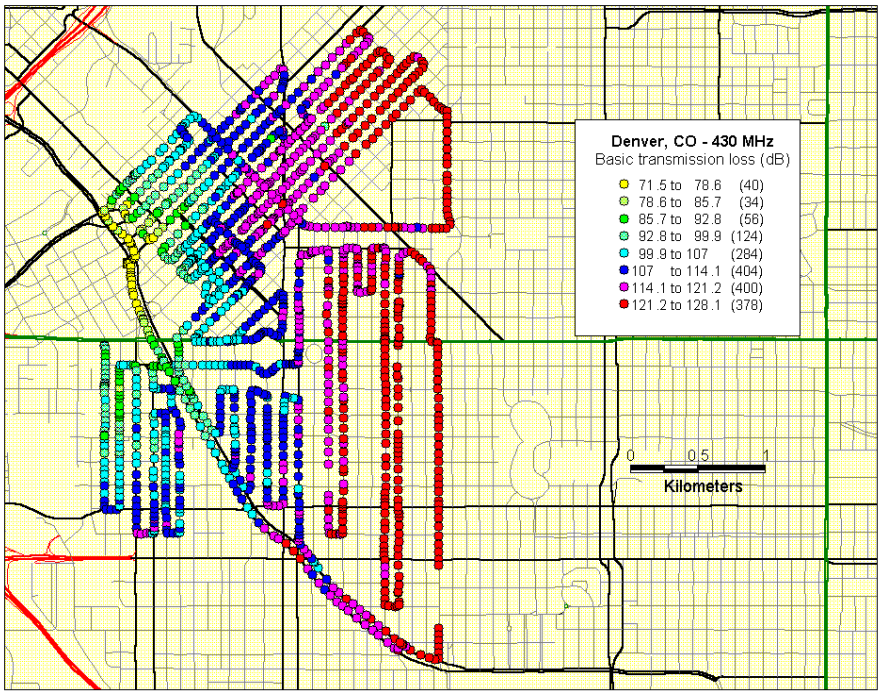

Figure 7. Basic transmission loss (L_b) at 430 MHz all routes for downtown Denver, CO.

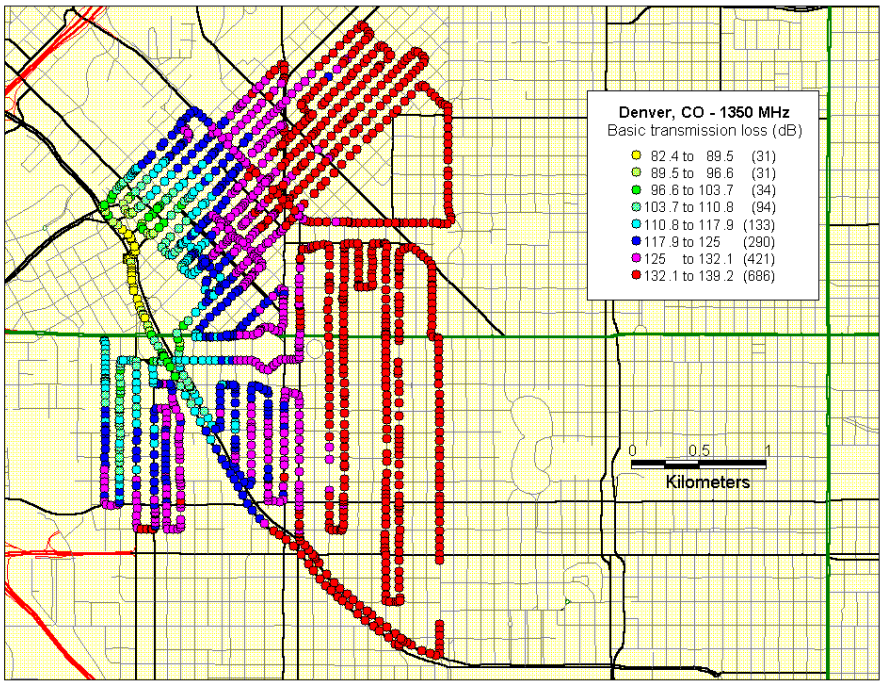

Figure 8. Basic transmission loss (L_b) at 1350 MHz all routes for downtown Denver, CO.

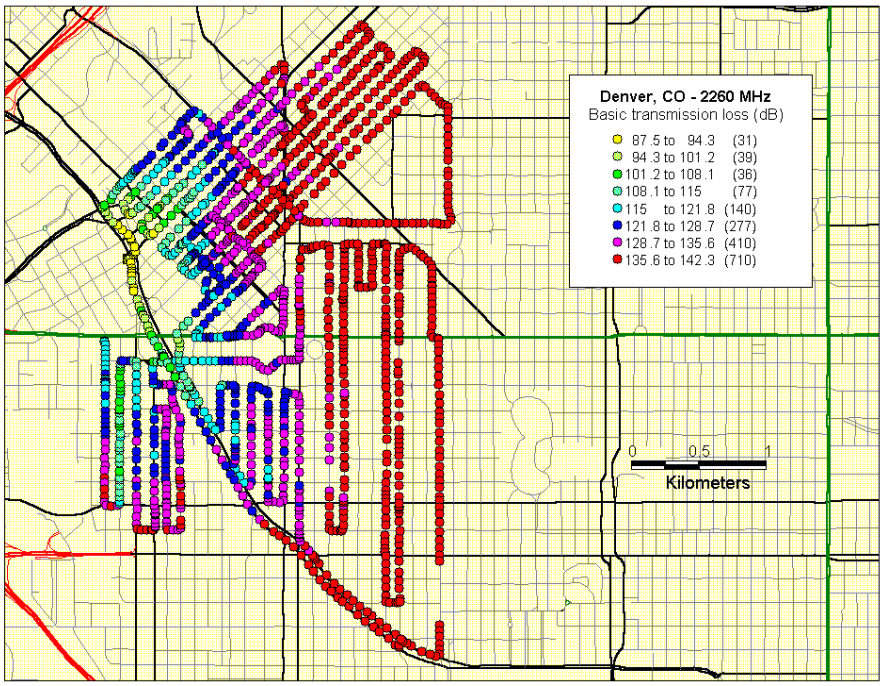

Figure 9. Basic transmission loss (L_b) at 2260 MHz all routes for downtown Denver, CO.

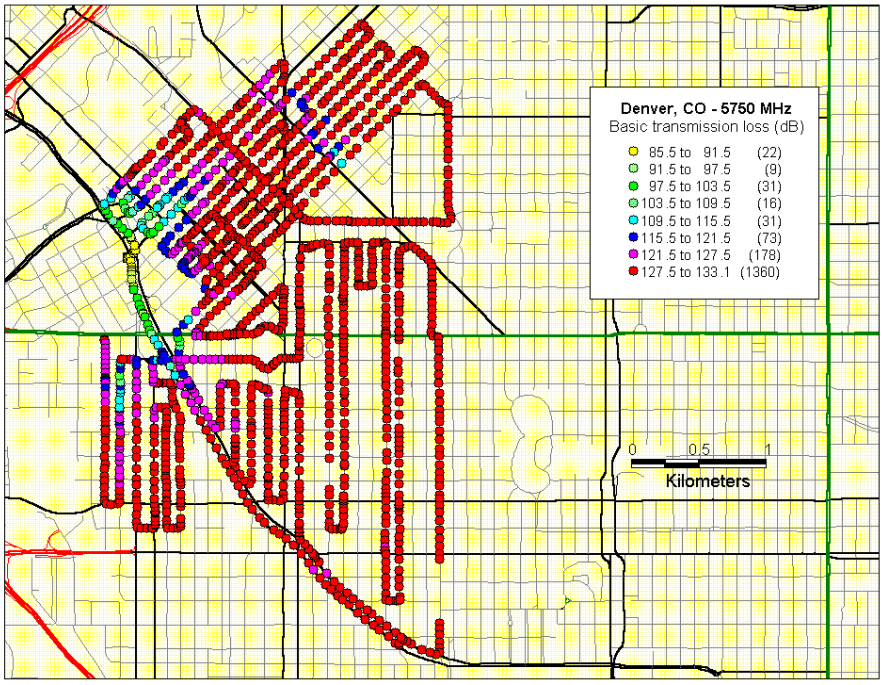

Figure 10. Basic transmission loss (L_b) at 5750 MHz all routes for downtown Denver, CO.

5.2 Basic Transmission Loss

L_b is the total loss in power between the transmitter and receiver antennas. It includes both the free space loss and loss due to attenuation. Comparing Figures 7 and 10 we can see large differences in L_b between 430 MHz and 5750 MHz. Close to the transmitter where there are line-of-sight conditions, L_b is between 70-80 dB at 430 MHz and 85-90 dB at 5750 MHz. This difference is due to the increase in free space spreading loss (L_{fs}) at 5750 MHz. At a distance of 1-2 km from the transmitter we no longer have line-of-sight conditions, and now signal attenuation due to diffraction and shadowing cause additional signal losses. At these distances L_b is between 85-90 dB at 430 MHz, while at 5750 MHz L_b is between 100-120 dB. L_b can be used to quantify the increased power requirements for high frequency systems needed to achieve the same level of signal coverage or cell size. Larger attenuation and basic transmission losses limit the range of higher frequency systems. This is apparent when comparing Figure 7 to Figure 10. The area with losses below 100 dB at 5750 MHz extends out to less than 1 km, while at 430 MHz this area extends to 2 km in many directions.

Data in this format, tagged with latitude and longitude coordinates, is useful for a comparison to modeling results, but it is difficult to use for quantitative comparisons versus frequency. To do this it is better to display L_b versus distance in scatter plots and measure the average slope and data distribution around a local mean. These methods and results are described in sections 5.3 and 5.4.

5.3 Basic Transmission Loss Slope

By plotting the basic transmission loss in dB versus *log* distance from the transmitter, L_b becomes a linear function (Figures 11-14). The average slope (dB/decade) for L_b can then be determined using a least squares fitting method. This data can be compared to free space loss (L_{fs}), the spreading loss for an isotropic signal with no obstructions. L_{fs} is a function of frequency and can be computed using Equation 8 where d is the distance between transmitter and receiver and λ is the carrier wavelength. Because L_b is the total loss in power between the transmitter and receiver it includes both L_{fs} and the signal attenuation (A) due to diffraction and shadowing. This relationship is given in Equation 9.

$$L_{fs} = \left(4\pi d \big/ \lambda\right)^2 \tag{8}$$

$$L_{bt}(dB) = L_{fs}(dB) + A(dB) \tag{9}$$

Another common metric, the loss exponent, can be computed by dividing the slope by 10. For instance, a slope of 40 dB/decade is equivalent to a slope exponent of 4. The slope of A can be determined by subtracting the free space loss slope of 20 from the L_b slope. Line-of-site propagation paths can be dominated by L_{fs} and have little loss due to signal

attenuation. These data points in urban areas will tend to be close to the transmitter and follow an L_{fs} trend line. Sometimes short path data points do not follow the L_{fs} trend line (close in red points on Figures 11-14). These points were shadowed by the transmitter building or are in the side lobes of the transmitting antenna pattern. In all the plots (after we get into the main antenna lobe) first we see a region near the transmitter where the slope of the L_b is near 20dB/decade ($10*log$ (L_{fs})). This region occurs within the first 100 and 300 m from the transmitter and indicates line-of-sight conditions.

We then see a second region where the average slope increases, indicating that the radio path has become obstructed. Values in this region ranged between 29 and 59 dB/decade (see Figures 11-14, B5-B19, and Table 5). Signal attenuation due to diffraction and shadowing are also frequency dependent and path loss slopes in built up areas tend to increase with increasing frequency. At large separations, data sometimes reach the sensitivity limit of the receiver. This limit is indicated when the data trend flattens out. These points are also marked in red and are not included in the trend line fit (see, e.g., Figures B6 and B8).

These trends are not clear for Sector 1 Route 2 (Figures B9-B12). Data from this route are very scattered and a trend line is visible for only a small region at short distances from the transmitter. This route covered urban low-rise, high-rise and line-of-sight areas. Consequently the data is too variable to be characterized using the average slope method and it was not possible to extract meaningful slope data. To decrease the variance, this data set was separated into two regions. One region is east of Speer Blvd. and is predominantly urban (see Figures B13-B16). The other region is west of Speer Blvd. and is a mixture of urban low-rise, residential and line-of-sight. The mixed urban data was not included in the analysis because it still had a large variability and much of the 5750 MHz data was unusable because the sensitivity limit of the receiver was surpassed (see Figures B17-B20).

Sector 2 Route 1 was predominantly urban high-rise. This data was also used for the average slope analysis to determine the relative nature of signal loss (L_b) versus frequency (Figures B21-B24). Data from this route displayed in Figure B24 also illustrate the effects of high frequency power amplifier limitations and the decreased sensitivity of the receiver at 5750 MHz.

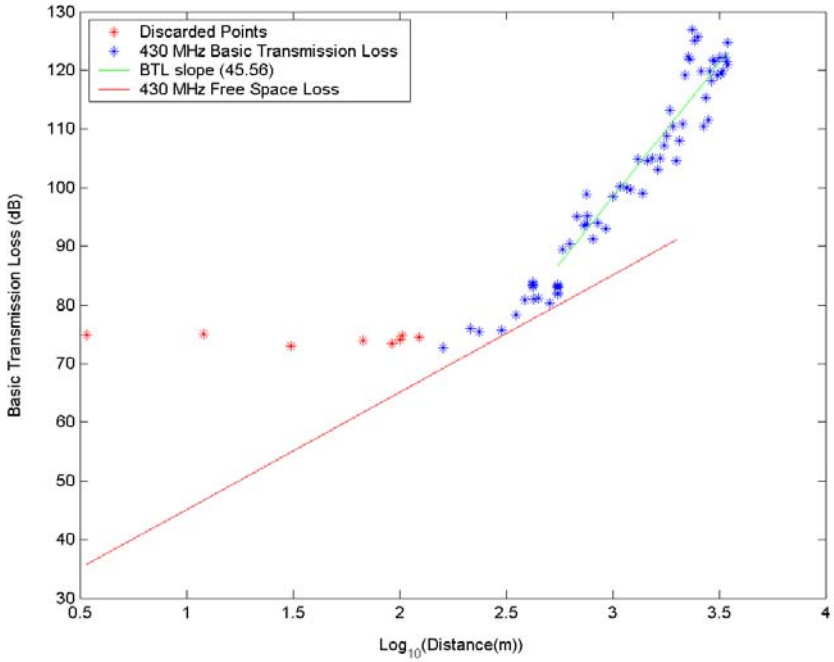

Figure 11. Basic transmission loss versus distance, sector 1 route 1, at 430 MHz.

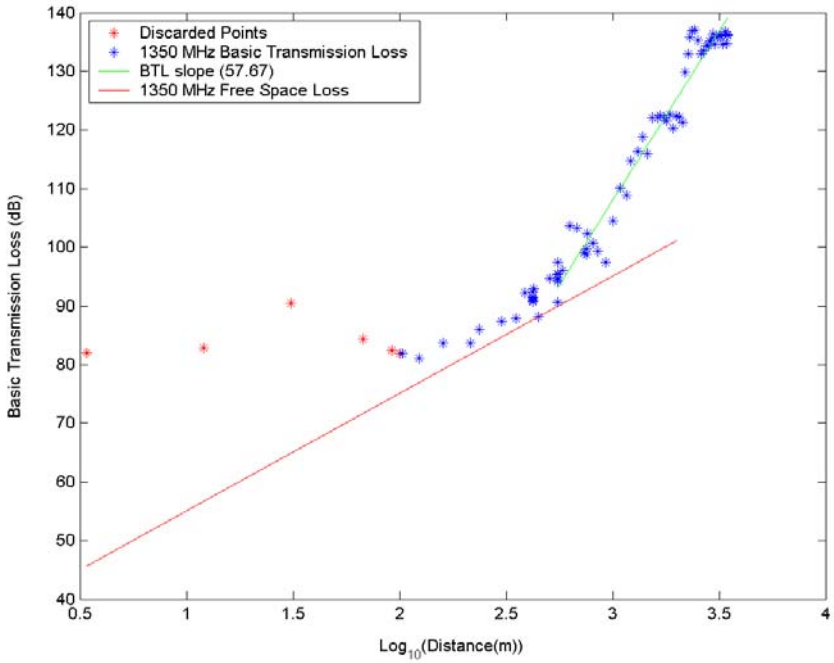

Figure 12. Basic transmission loss versus distance, sector 1 route 1, at 1350 MHz.

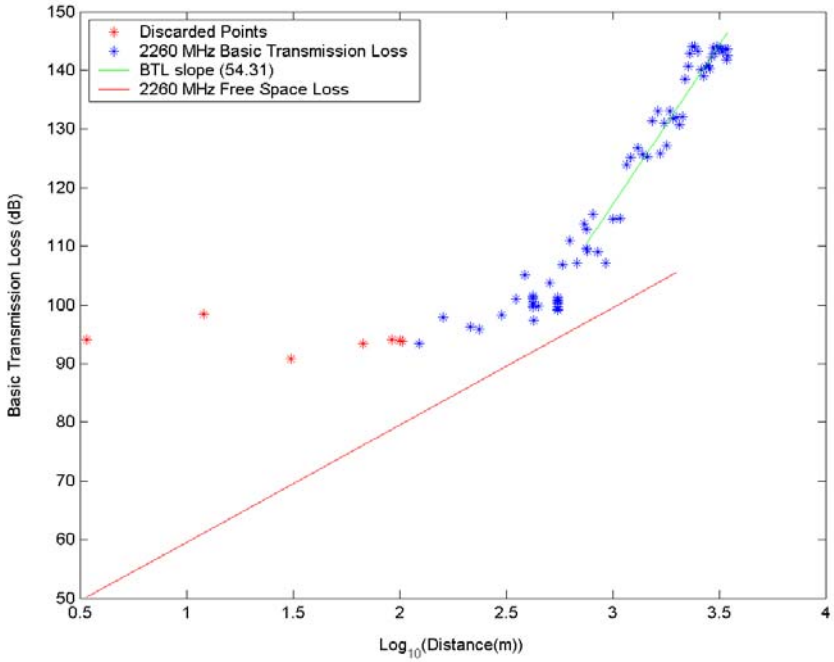

Figure 13. Basic transmission loss versus distance, sector 1 route 1, at 2260 MHz.

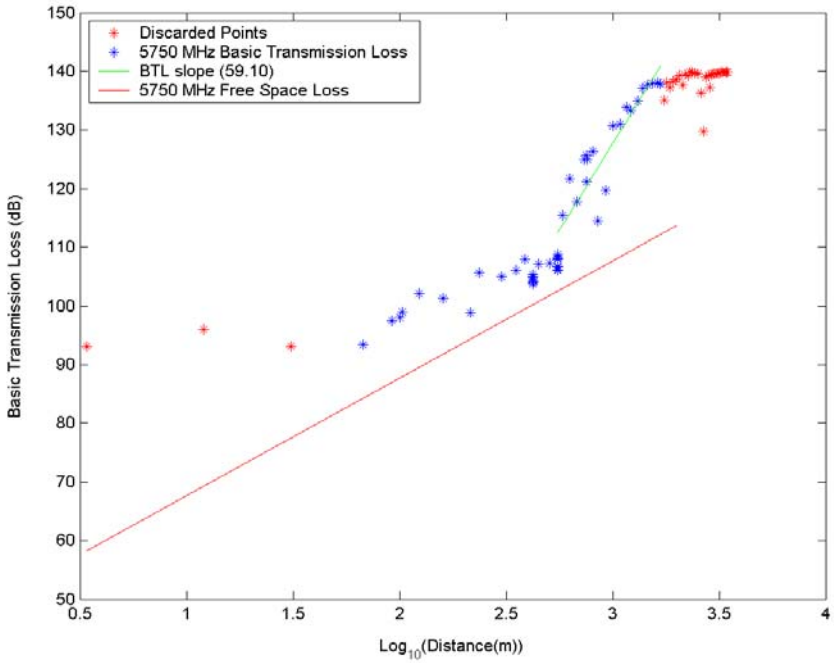

Figure 14. Basic transmission loss versus distance, sector 1 route 1, at 5750 MHz.

L_b and attenuation (A) slopes are summarized in Tables 5 and 6, respectively. The distance where line-of-sight communications is lost will depend upon the transmitter location and height. The average signal loss beyond this distance can be estimated using the slopes in Table 5. Although we see large route-to-route variability at any one

frequency, the trend to larger path loss slopes at higher frequencies is consistent on all routes. The increase in L_b slope between 430 MHz and 5750 MHz is between 9 and 14 dB/decade, while the increase between 2260 and 5750 MHz is between 1 and 5 dB/decade with an average of 3.5 dB. Path loss slope versus frequency is plotted in Figure 15. The average slope increase is about 11 dB/decade and is approximately linear over the decade of frequencies between 430 MHz and 5750 MHz.

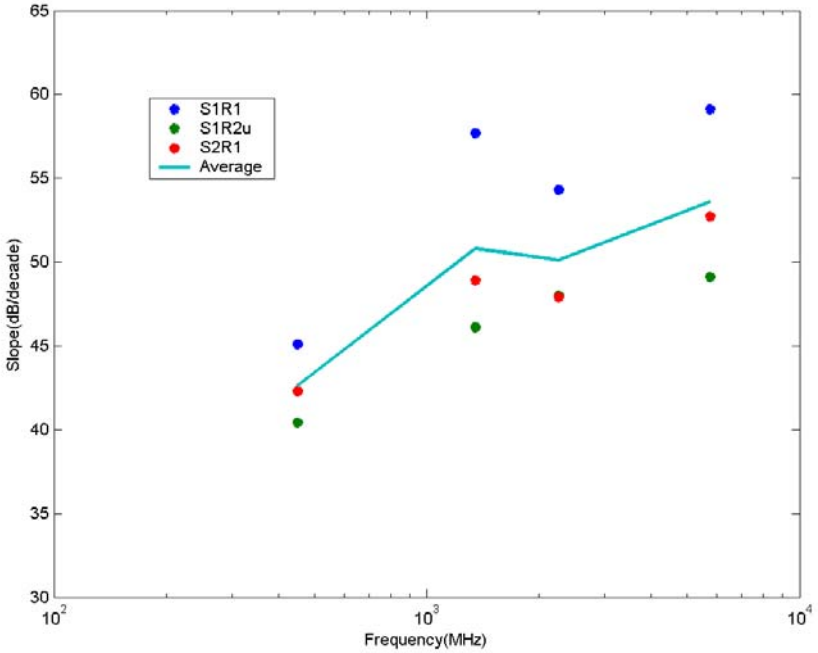

Figure 15. L_b slope versus frequency for three urban drive routes in Denver, CO.

For comparison, several measured and predicted PCS path loss exponents from Steele [5] are summarized in Table 7. These measurements are from an urban environment in southern England using 1.8 GHz narrowband data averaged over 6.44 m (38λ). The base antenna height was varied between 6 m and 14 m and the receiver antenna height was 2 m. Measured results from this survey in England predict lower average path loss slope than those reported here. While predictions using the HATA model are higher than the Steele measurements, our survey measured still larger path loss slopes at all frequencies predicted using the HATA model. In fairness to the HATA model, in both cases the model is applied beyond its original frequency range. In addition, there is a strong dependence on measurement environment and survey geometry that makes comparison of measurements collected in different environments difficult.

Our data were collected simultaneously at the same measurement points and the relative nature of our results is consistent for different routes in our survey. Given this, the average value of the relative measurements should be applicable to urban areas.

Table 5. L_b Slopes for Three Routes in the Downtown Area of Denver, CO

	$\Delta L_b / \Delta r$ (dB/decade)			
Route	430 MHz	1350 MHz	2260 MHz	5750 MHz
S1R1	45.1	57.7	54.3	59.1
S1R2/urban	40.4	46.1	48.0	49.1
S2R1	42.3	48.8	47.9	52.7
Average	42.6	50.8	50.1	53.6

Table 6. Summary of Attenuation Slopes for Three Routes in the Downtown Area of Denver, CO

	ΔA (dB/decade)			
Route	430 MHz	1350 MHz	2260 MHz	5750 MHz
S1R1	25.1	37.7	34.3	39.1
S1R2/urban	20.4	26.1	28.0	29.0
S2R1	22.3	28.8	27.9	32.7
Average	22.6	30.9	30.1	33.6

Table 7. L_b Slopes Measured at 1850 MHz in an Urban Area of Southern England and Predictions Made Using the Hata Model

Antenna Height (m)	Measured ΔL_b (dB/decade)	Hata Slope (dB/decade)	Slope Difference (dB/decade)
14	24.6	37.4	-12.8
11.4	29.8	38	-8.2
8.9	34.5	38.7	-4.2
6.4	36.3	39.6	-3.6

5.4 Lognormal Statistics

The path loss slope is used to describe the average signal loss versus distance, and the probability of receiving a signal at this average level is described statistically. It has been observed that variability of communication signals above or below the average signal or local mean can be described using a lognormal distribution with a standard deviation σ [6]. Both of the metrics, L_b and σ, have been observed to be dependent upon the environment and frequency of the radio signal. To verify that our data follows this observed trend, the cumulative distribution function (CDF) of the difference between the measured basic transmission loss and the mean path loss is plotted on lognormal probability paper in Figures 16 and 17. By using lognormal probability paper the CDF will be linear if the data is normally distributed around the local mean. On both figures, the data follows the lognormal trend line. The slope of these graphs is equal to the standard deviation (σ) of the distribution. In Figure 16 the data for the urban high-rise route (S2R1) is plotted and σ varies from 4.6 at 430 MHz, 4.4 at 1350 MHz, 5.3 at 2260 MHz, and 5.9 at 5750 MHz. These results are similar to measurements reported in Tokyo by Okumura [7] and in London by Ibrahim [8]. Okumura found σ varied between 3 dB and 7 dB. Ibrahim measured σ's of 5 dB at 168 MHz, 5.65 dB at 455 MHz, and 6.4 dB at 900 MHz. In Figure 16 (urban high-rise), we see increasing σ with frequency and higher values than in Figure 17, which has data from an urban low-rise area as well as a large

open boulevard. In this area we see lower values of σ ranging from 3.3 to 4.2 dB but with no trend versus frequency.

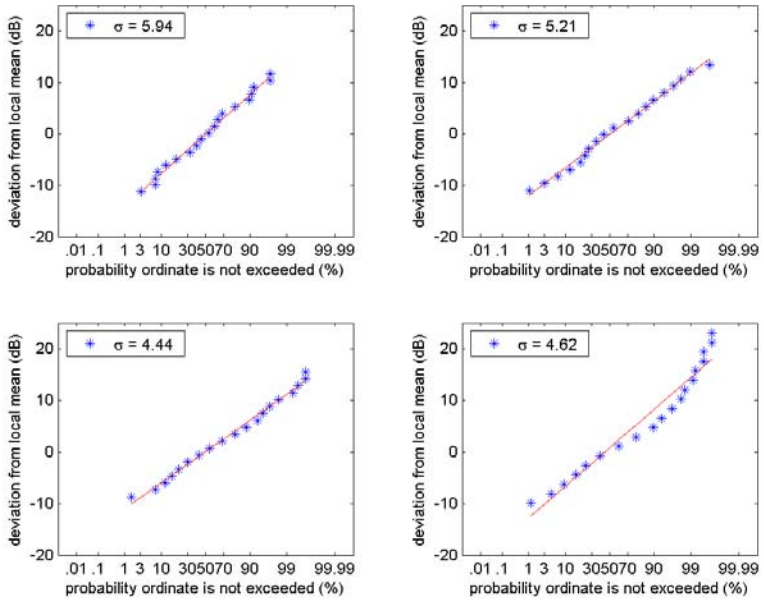

Figure 16. Basic transmission loss distribution about the local mean plotted on lognormal paper for the urban high-rise (S2R1) environment in downtown Denver, CO. Data for four frequencies are plotted: (a) 5750 MHz, (b) 2260 MHz, (c) 1350 MHz, and (d) 430 MHz.

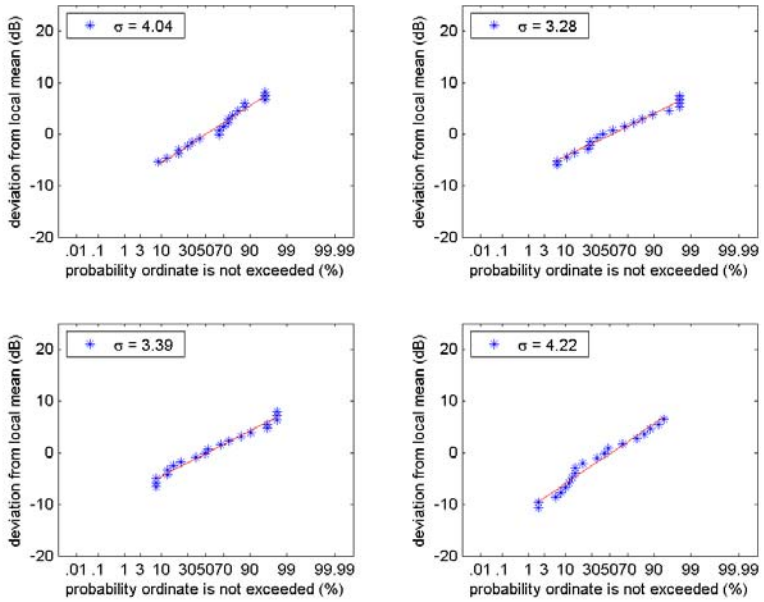

Figure 17. Basic transmission loss distribution about the local mean plotted on lognormal paper for an urban low-rise (S1R1) environment near downtown Denver, CO. Data for four

frequencies are plotted: (a) 5750 MHz, (b) 2260 MHz, (c) 1350 MHz, and (d) 430 MHz.

5.5 Delay Statistics

S values versus GPS coordinates are displayed in map view in Figures B1-B4. For quantitative analysis the cumulative distribution function (CDF) of delay spreads is used. In Figures 18 and B25-B29 the CDF's for different drive routes at the four frequencies are plotted. The CDF's allow one to determine the percentage of signals whose delay spread is larger than the abscissa value. We can see that lower frequencies exhibit a higher probability of larger delay spreads on all routes, especially in the urban areas such as in sector 1 route 2 and in sector 2.

The smaller delay spreads indicate that the high frequency reflected signals were attenuated and fell below the 20 dB cutoff used for delay spread calculations.

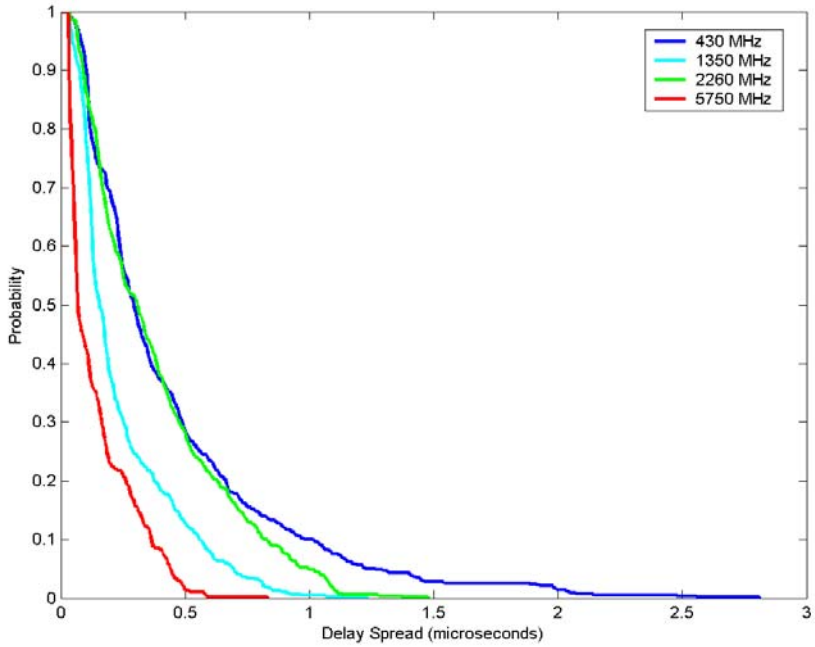

Figure 18. Cumulative distribution of delay spreads, sector 1 route 1, 430-5750 MHz.

On Figure 19 we have plotted the median *S* for different drive routes and the average median *S* for all routes. The 10% quantile data for *S* is plotted on Figure B30. In both figures we see a trend indicating an almost linear decrease in *S* over the decade of measurement frequencies. This trend is clearer for the average value of *S* over all drive routes than the readings for individual drive routes. Delay spread and maximum delay values are summarized at these two quantiles in Tables 8 and 9. We see that the average median delay spread decreased from 0.7 to 0.27 μs between 430 MHz and 5750 MHz. The maximum delay is less predictable but also appears to decrease at increased frequency.

Table 8. Delay Spread Cumulative Distribution Summary at 50% and 10% Quantiles by Drive Routes with Averages

Ordinate Exceeded	*S (μs) 50%*				*S (μs) 10%*			
Frequency (MHz)	430	1350	2260	5750	430	1350	2260	5750
S1R1	0.3	0.2	0.3	0.1	.95	0.6	0.8	.35
S1R2	0.9	.85	0.8	0.3	1.3	1.4	1.4	1.0
S2R1	0.8	.75	0.7	0.4	1.2	1.3	1.2	0.7
Average	0.7	0.6	0.6	.27	1.2	1.1	1.1	.68

Table 9. Maximum Delay Cumulative Distribution Summary at 50% and 10% Quantiles by Drive Route with Averages

Ordinate Exceeded	*Maximum Delay 50%*				*Maximum Delay 10%*			
Frequency (MHz)	430	1350	2260	5750	430	1350	2260	5750
S1R1	5.5	4.0	4.0	3.0	14	9.5	12	6.0
S1R2	9.0	9.0	9.0	6.0	13	12	12.5	7.5
S2R1	8.5	8.0	7.0	4.0	11	11	10	6.0
Average	7.7	7.0	9.0	6.7	13	11	11	6.5

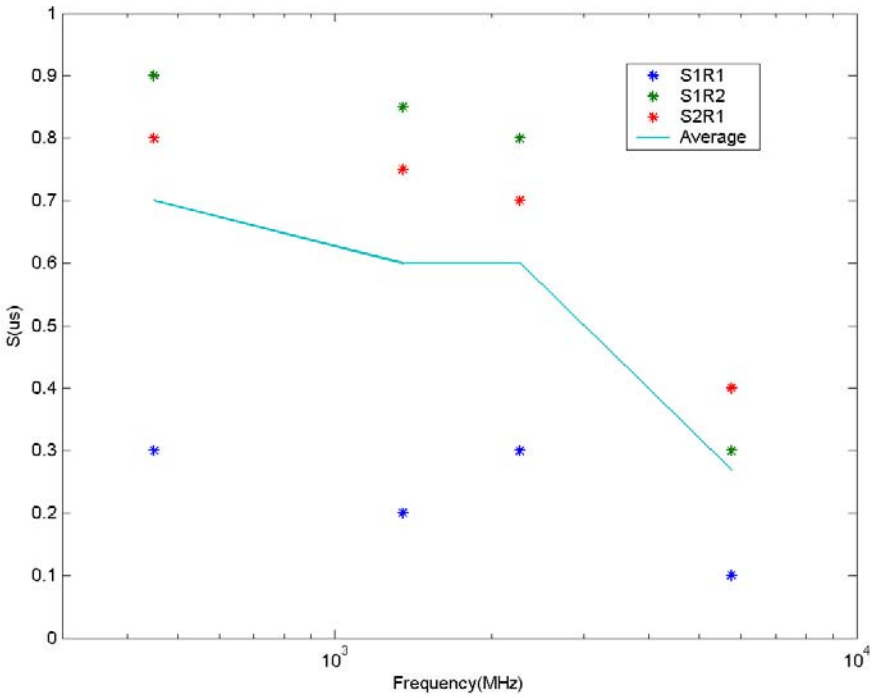

Figure 19. Median delay spreads versus frequency for each sector and route.

6. CONCLUSIONS

Data from a propagation survey in Denver were analyzed to determine the relative propagation impairments over the decade of frequencies from 430 MHz to 5750 MHz. Wideband received power data were analyzed to determine the path loss slope increase as the carrier frequency was increased in an urban mobile setting. The data were also analyzed to determine if L_b was normally distributed about the average path loss and what the deviation was. It was found that the path loss slope on average increased from 43 to 54 dB/decade between 430 and 5750 MHz in an urban environment. The average increase in path loss slope between 2260 and 5750 MHz was 3.5 dB and ranged from 1 to 5 dB. The data were normally distributed and σ ranged between 3 and 6 dB, consistent with previously reported measurements. In contrast to this trend, the delay spread decreased at higher frequencies. It was found that the median delay spread decreased from 0.7 μs to 0.3 μs and the 10% exceedance quantile decreased from 1.2 μs to 0.8 μs indicating a 35% to 60% decrease in delay spread. This decrease in delay spread is beneficial for high data rate transmissions and could offset the propagation impairments caused by larger path loss and power amplifier limitations at high frequency.

7. ACKNOWLEDGMENTS

I would like to thank NTIA for supporting this research. I would also like to acknowledge Lucas Howell. Lucas was a summer intern at ITS between his junior and senior years at the University of Wyoming. He developed many of the computer processing programs used to analyze the propagation data in this report.

8. REFERENCES

[1] J.A. Wepman, J.R. Hoffman, L.H. Loew and V.S. Lawrence, "Comparison of wideband propagation in the 902-928 and 1850-1990 MHz bands in various macrocellular environments," NTIA Report 93-299, Sep. 1993.

[2] P.F. Wilson, P.B. Papazian, M.G. Cotton, and Y. Lo, "Advanced antenna test bed characterization for wideband wireless communications," NTIA Report 99-369, Aug. 1999.

[3] P.B. Papazian, Y. Lo, J.J. Lemmon and M.J. Gans, "Measurements of channel transfer functions and capacity calculations for a 16x16 BLAST array over a ground plane," NTIA Report TR-03-403, Jun. 2003.

[4] D. Parsons, *The Mobile Radio Propagation Channel*, NY: Halsted Press, 1994, pp.149-153.

[5] R. Steele, *Mobile Radio Communications*, Piscataway, NJ: IEEE Press, 1995, pp.160-163.

[6] D.O. Redunk, "Comparison of radio transmissions at X-band frequencies in suburban and urban areas," *IEEE Trans. Antennas and Propagation, AP-20*, pp. 470-473, 1972.

[7] Y. Okumura, "Field strength and its variability in VHF and UHF land mobile radio service," *Review Elec. Comm., Lab.,* 16, No. 9-10, pp. 825-873, 1968.

[8] M.F. Ibrahim, "Signal strength prediction for mobile radio communications in built up areas," Ph.D thesis, University of Birmingham, 1981.

APPENDIX A: DATA FILE SUMMARY

A list of the data files grouped by sector and drive route is given in Table A1. Each data file contains four channels of data, one for each carrier frequency. Text data files separate data for urban and mixed urban sections of sector 1 route 2.

Table A1. Raw Data File Information

Sector	Route	Transmitter Boresight	File
1	1 (Speer Blvd Southbound)	S45°E	507-516.br
1	1 (Speer Blvd Northbound)	S45°E	517-524.br
1	2	S45°E	525-625.br
2	1	N45°E	628-690.br
1	2 (urban, Speer East Side)	S45°E	Freq_urban.txt
1	2 (mixed, Speer West Side)	S45°E	Freq_mixed.txt

APPENDIX B: FIGURES

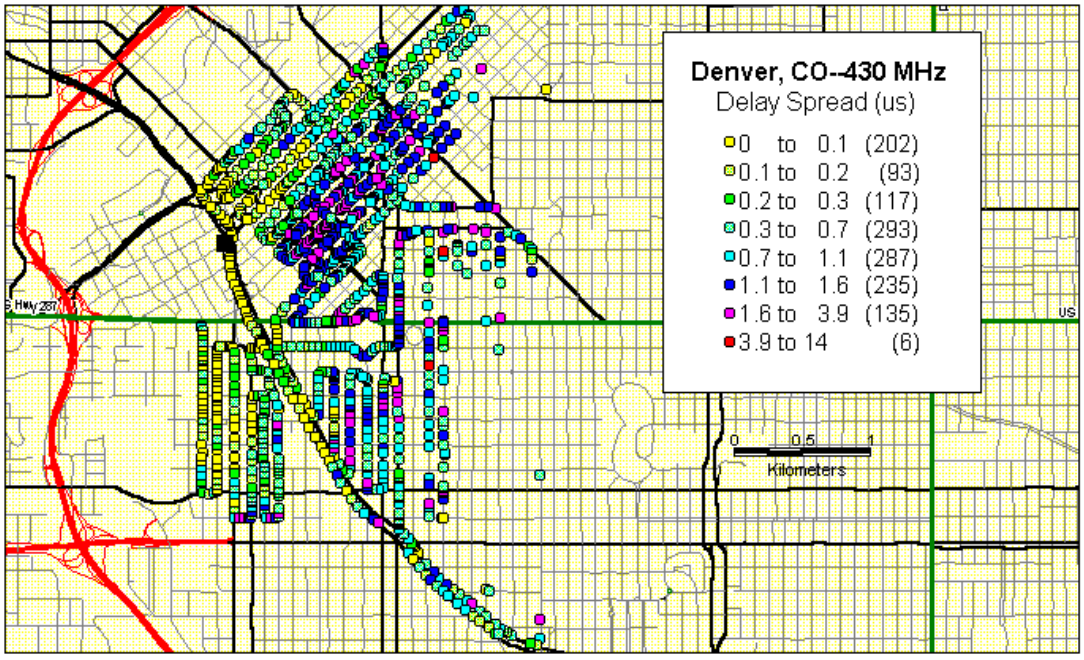

Figure B1. Measured delay spread (*S*) at 430 MHz all routes for downtown Denver, CO.

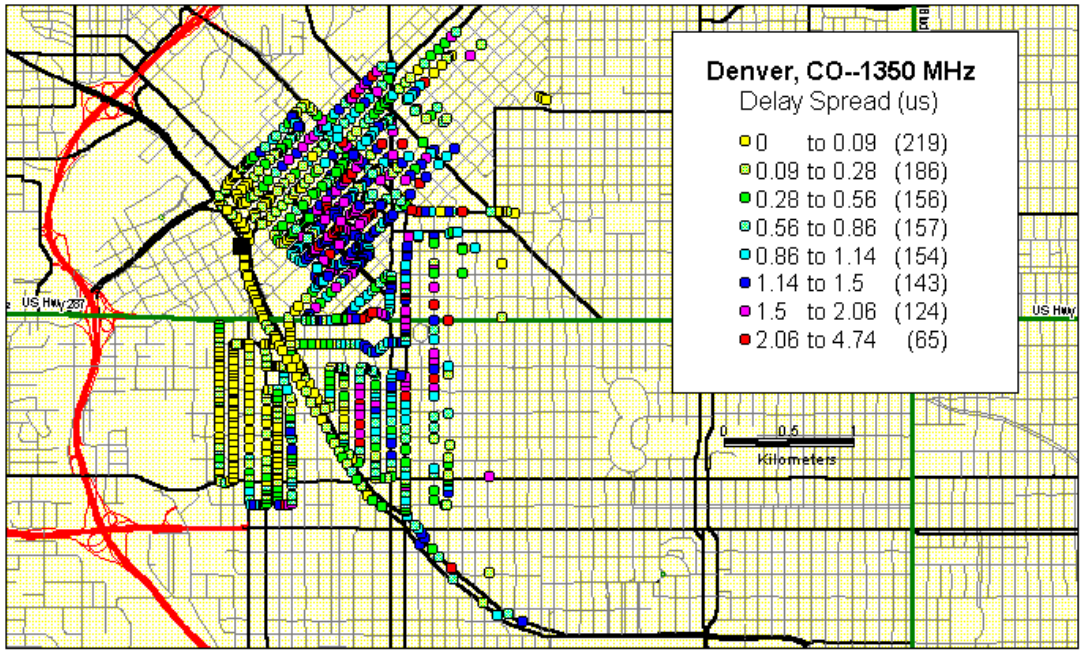

Figure B2. Measured delay spread (*S*) at 1350 MHz all routes for downtown Denver, CO.

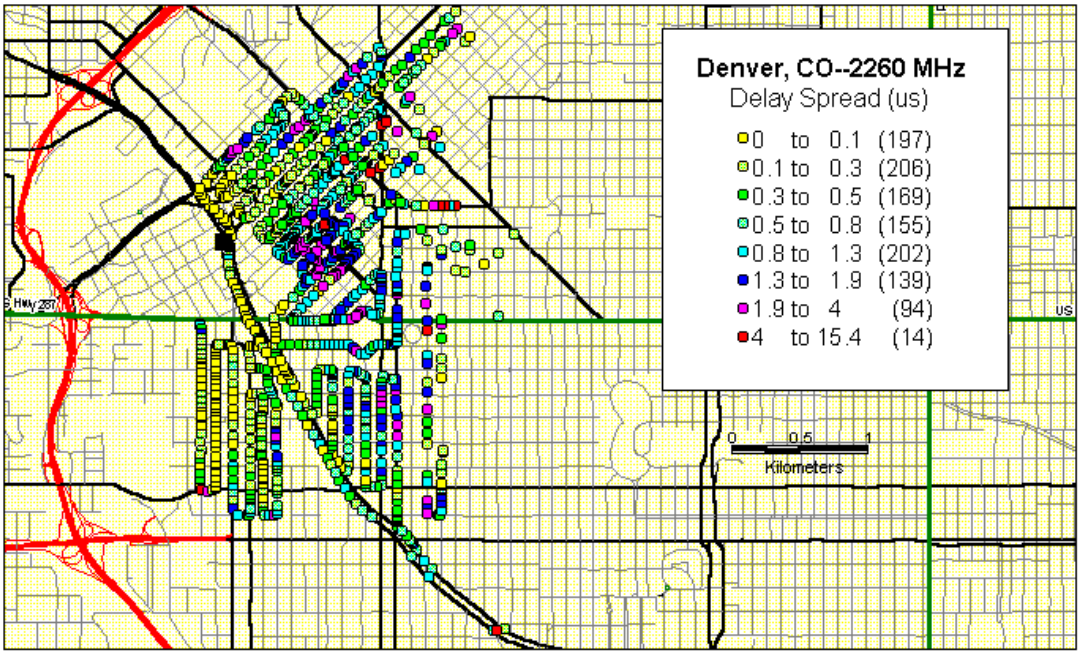

Figure B3. Measured delay spread (*S*) at 2260 MHz all routes for downtown Denver, CO.

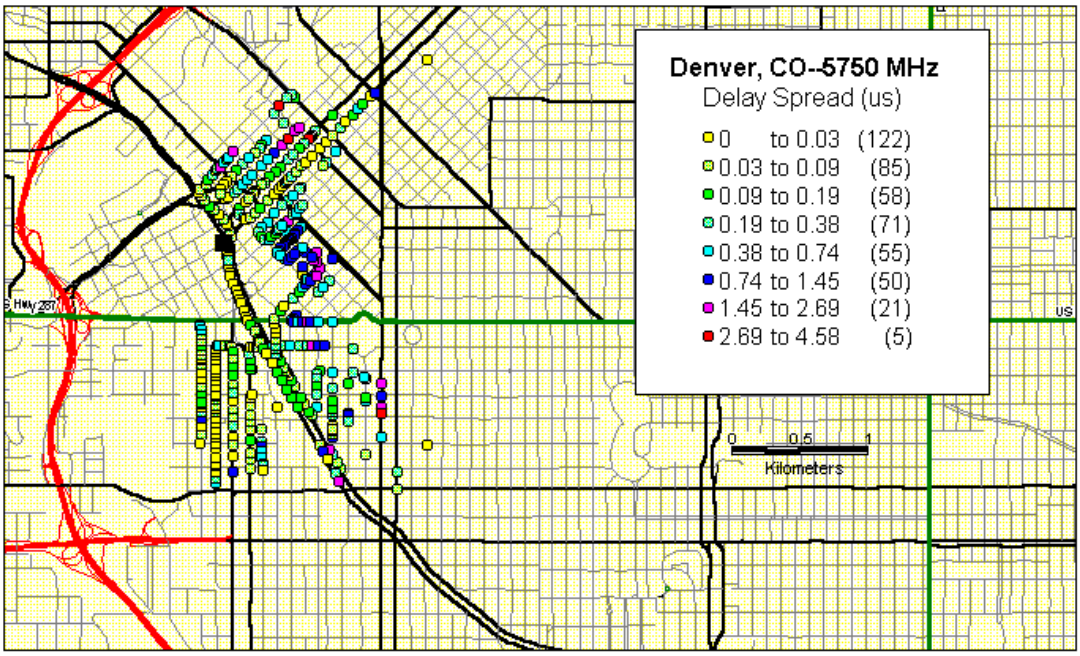

Figure B4. Measured delay spread (*S*) at 5750 MHz all routes for downtown Denver, CO.

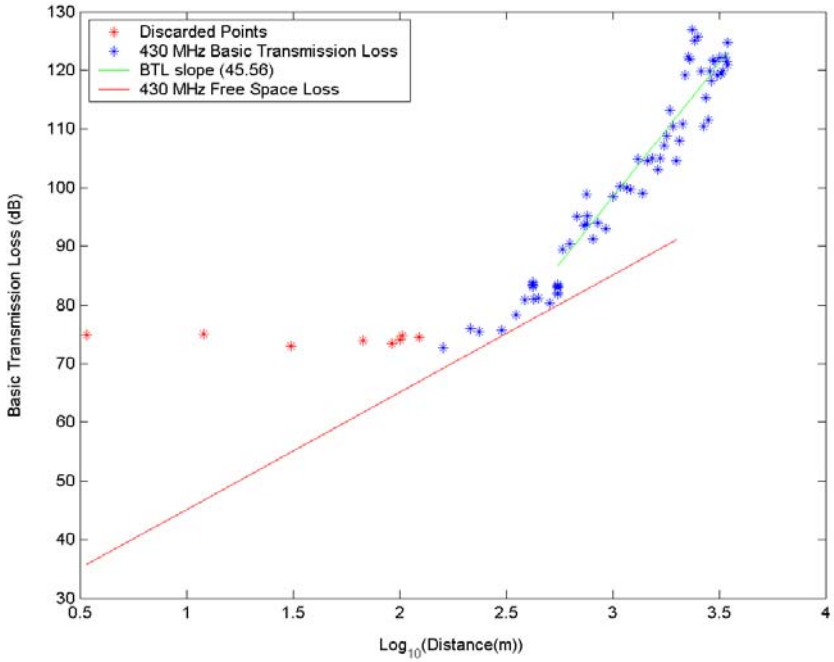

Figure B5. Basic transmission loss versus distance, sector 1 route 1, at 430 MHz.

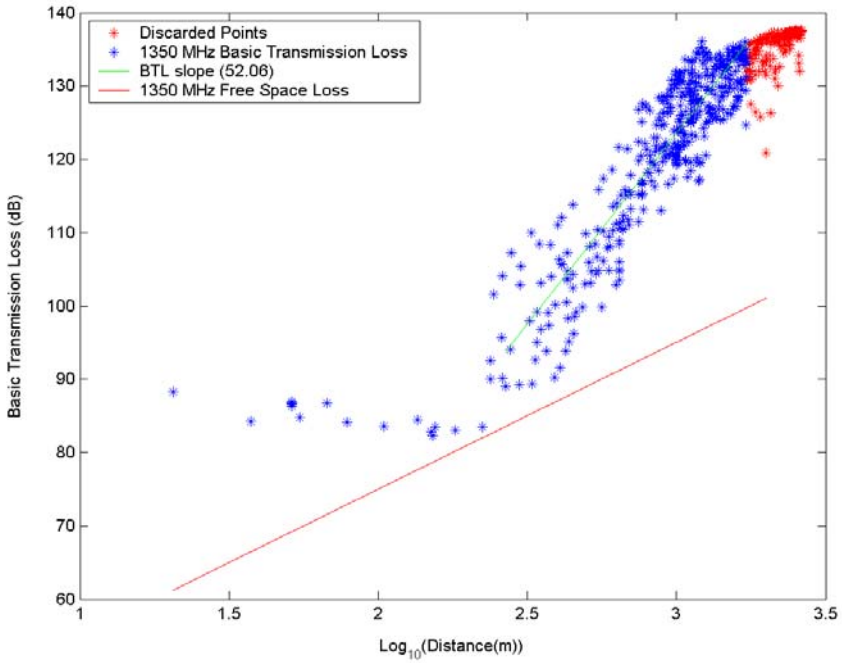

Figure B6. Basic transmission loss versus distance, sector 1 route 1, at 1350 MHz.

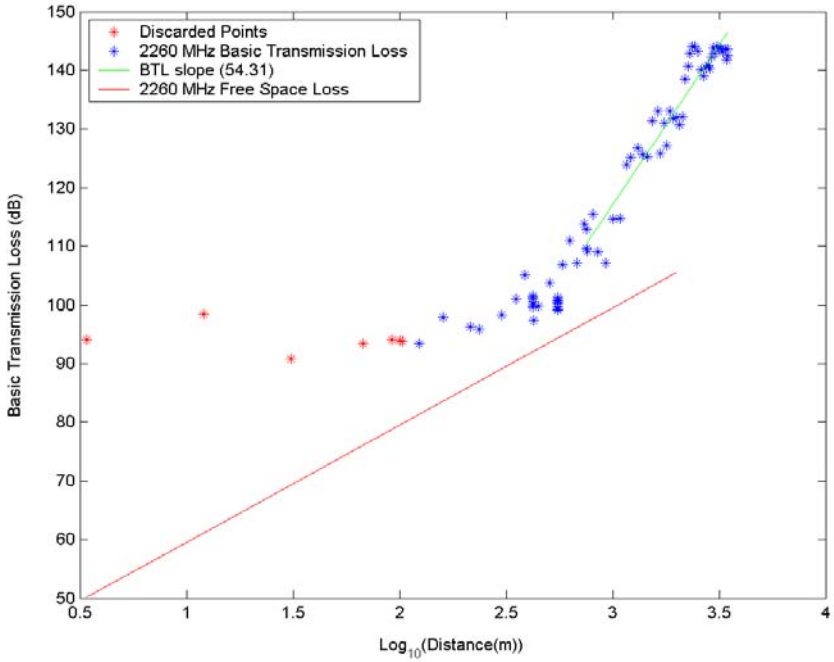

Figure B7. Basic transmission loss versus distance, sector 1 route 1, at 2260 MHz.

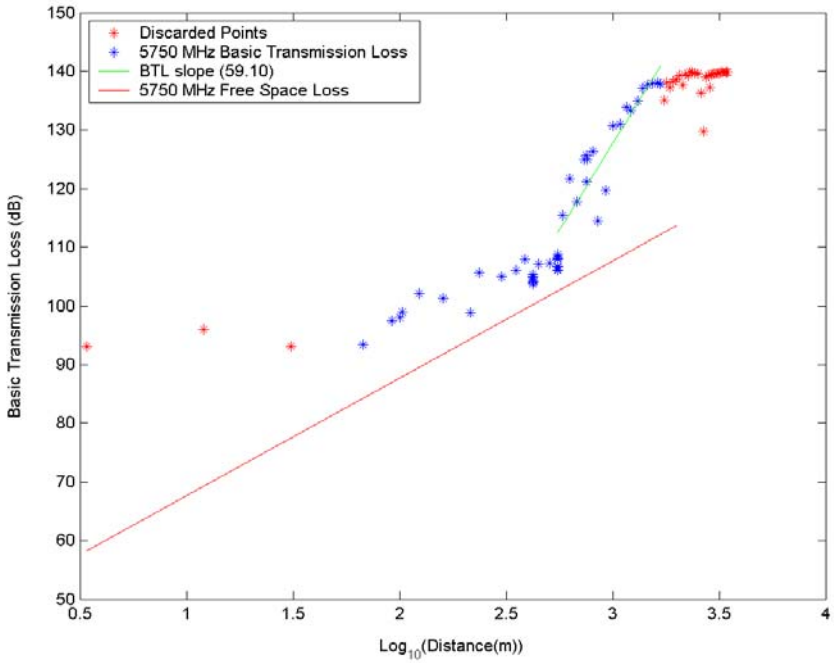

Figure B8. Basic transmission loss versus distance, sector 1 route 1, at 5750 MHz.

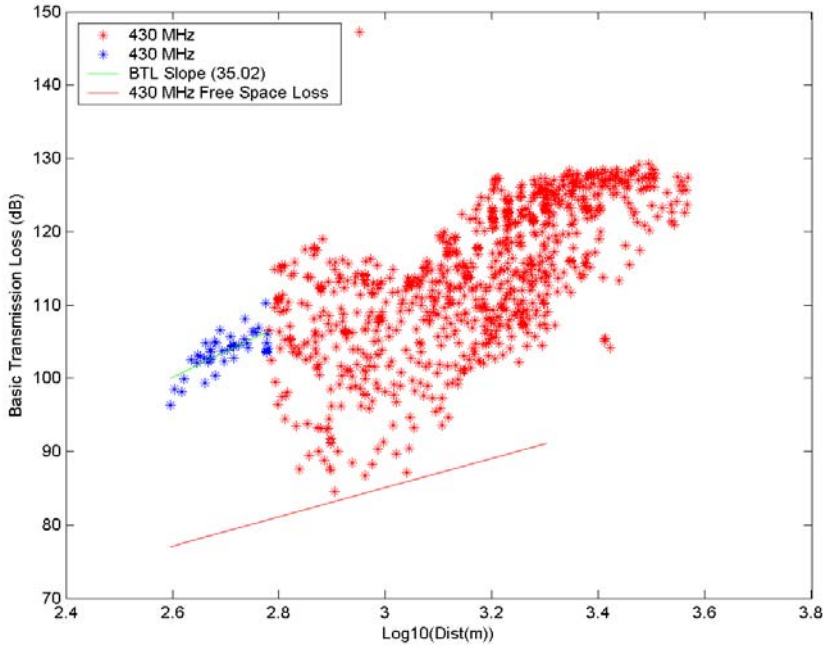

Figure B9. Basic transmission loss versus distance, sector 1 route 2, mixed urban low-rise and urban high-rise, at 430 MHz.

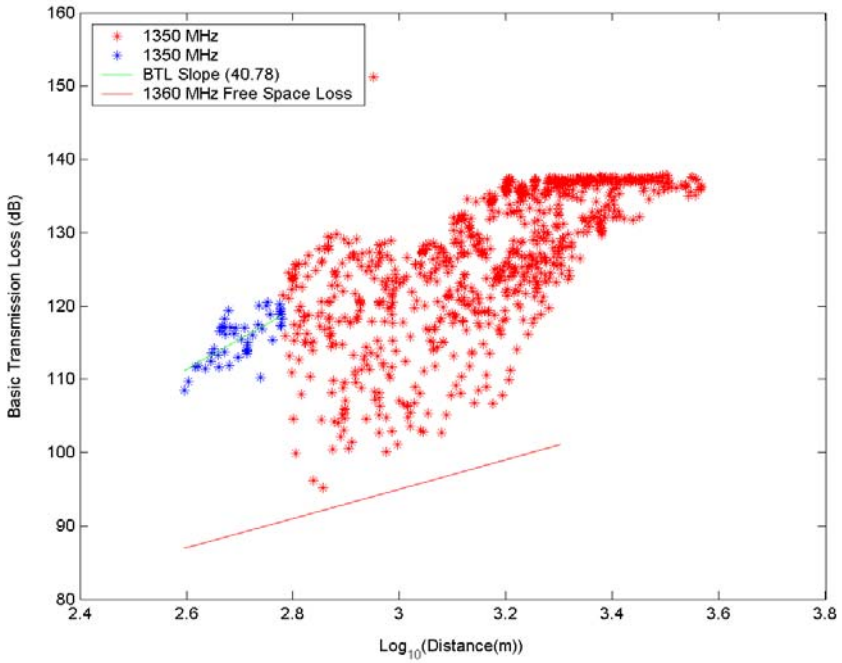

Figure B10. Basic transmission loss versus distance, sector 1 route 2, mixed urban low-rise and urban high-rise, at 1350 MHz.

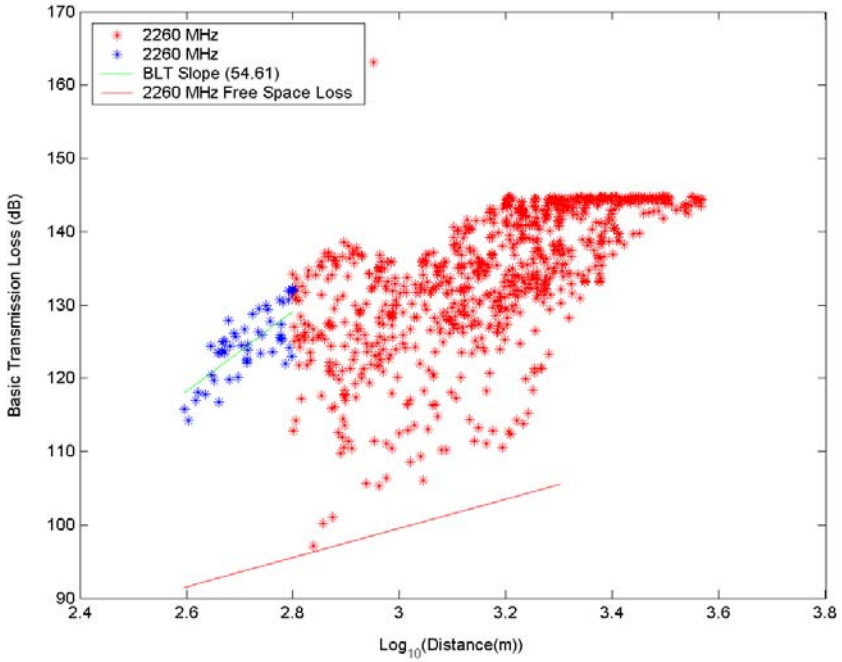

Figure B11. Basic transmission loss versus distance, sector 1 route 2, mixed urban low-rise and urban high-rise, at 2260 MHz.

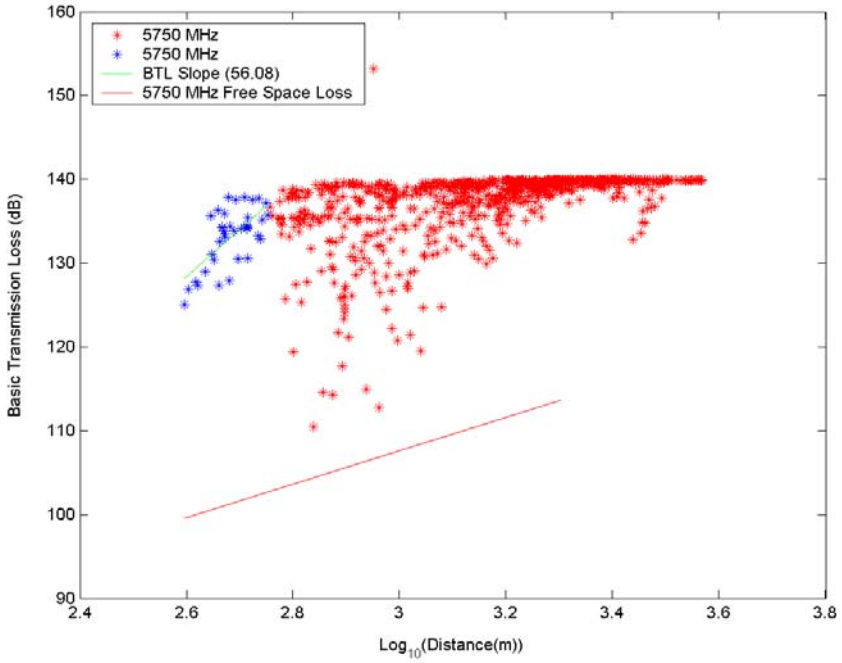

Figure B12. Basic transmission loss versus distance, sector 1 route 2, mixed urban low-rise and urban high-rise, at 5750 MHz.

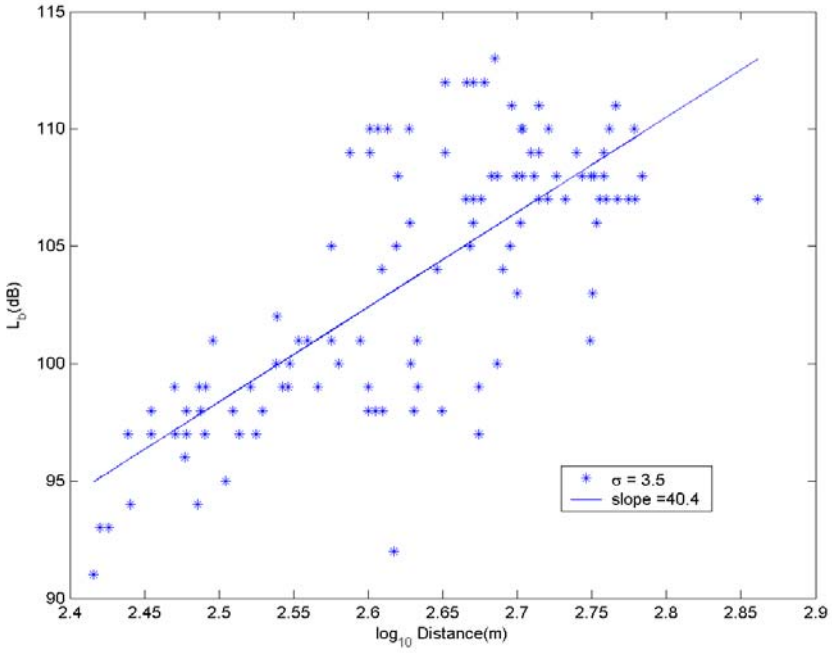

Figure B13. Basic transmission loss versus distance, sector 1 route 2, urban, at 430 MHz.

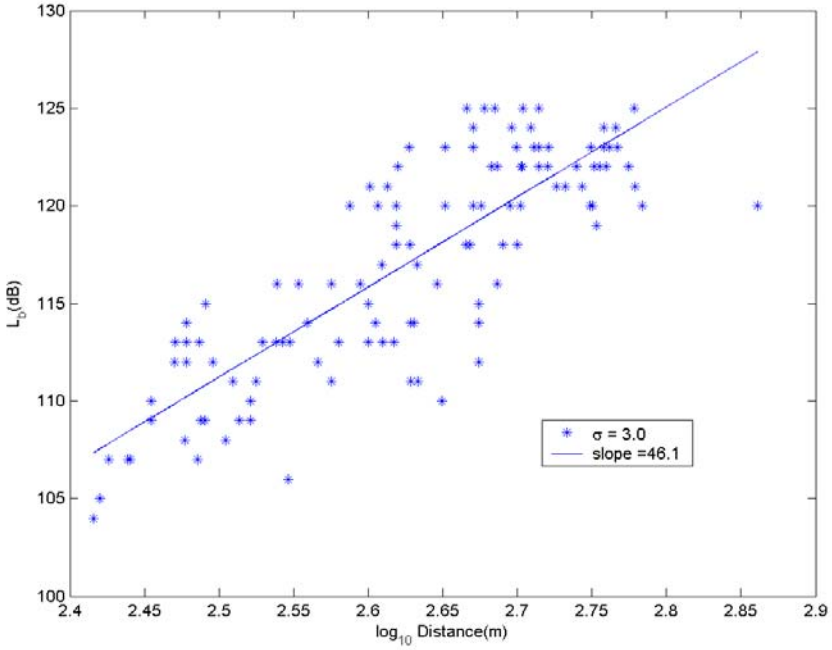

Figure B14. Basic transmission loss versus distance, sector 1 route 2, urban, at 1350 MHz.

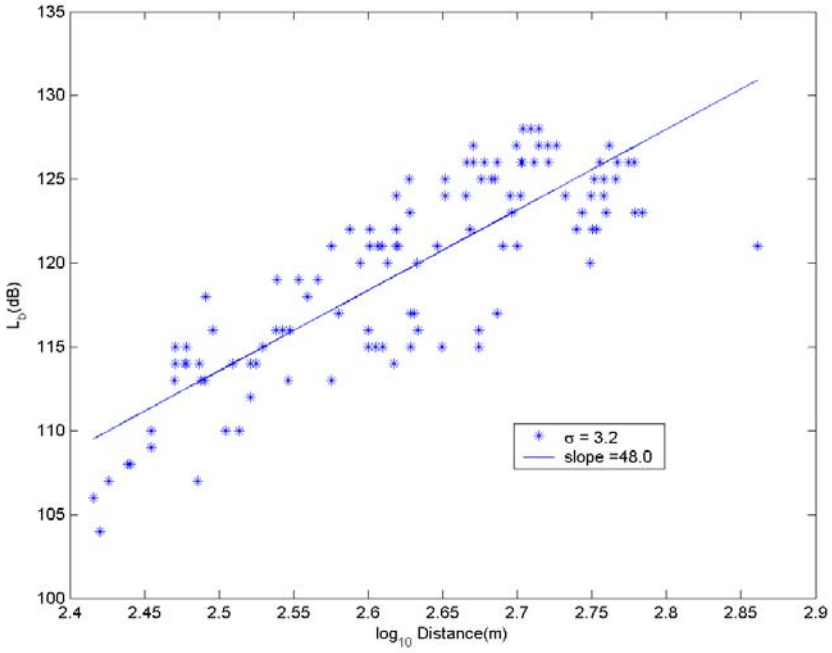

Figure B15. Basic transmission loss versus distance, sector 1 route 2, urban, at 2260 MHz.

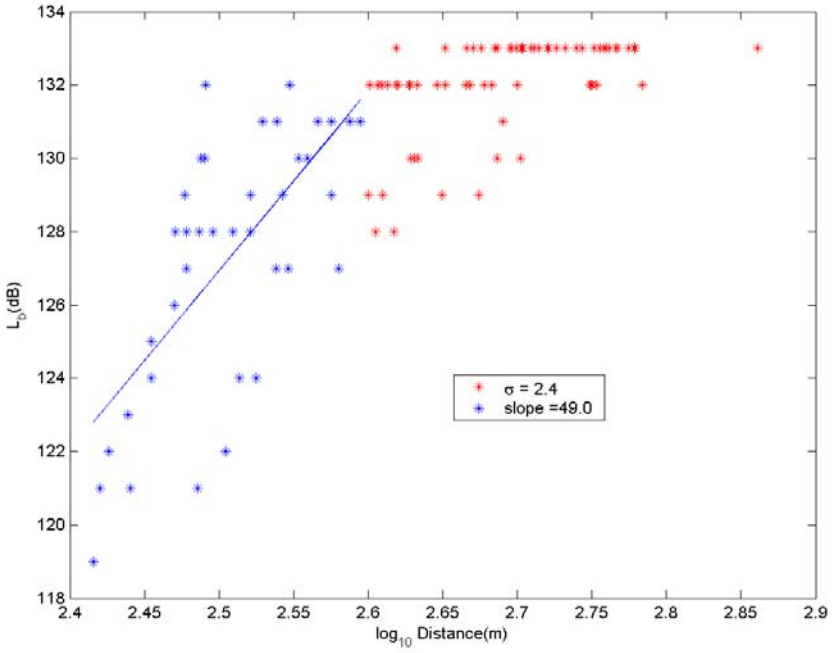

Figure B16. Basic transmission loss versus distance, sector 1 route 2, urban, at 5750 MHz.

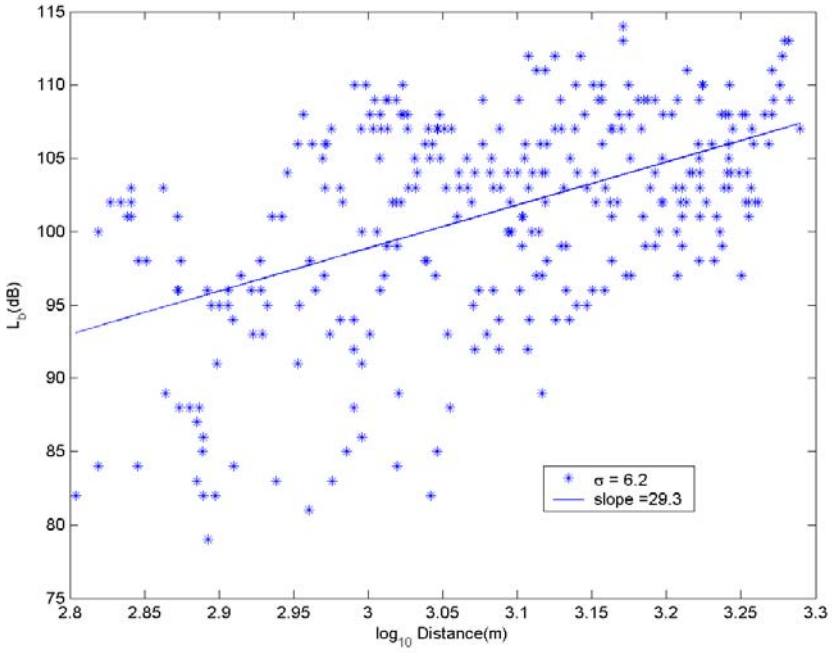

Figure B17. Basic transmission loss versus distance, sector 1 route 2, urban mixed, at 430 MHz.

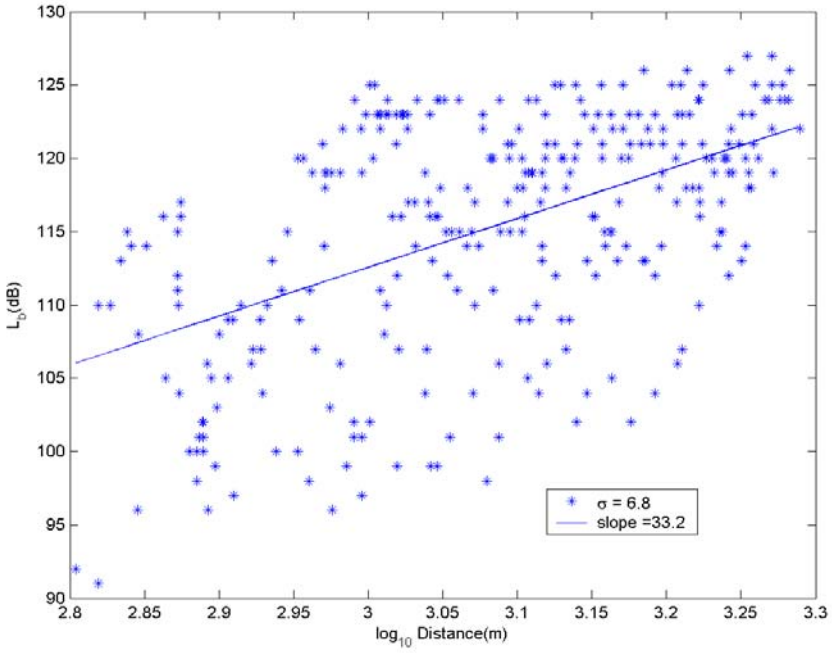

Figure B18. Basic transmission loss versus distance, sector 1 route 2, urban mixed, at 1350 MHz.

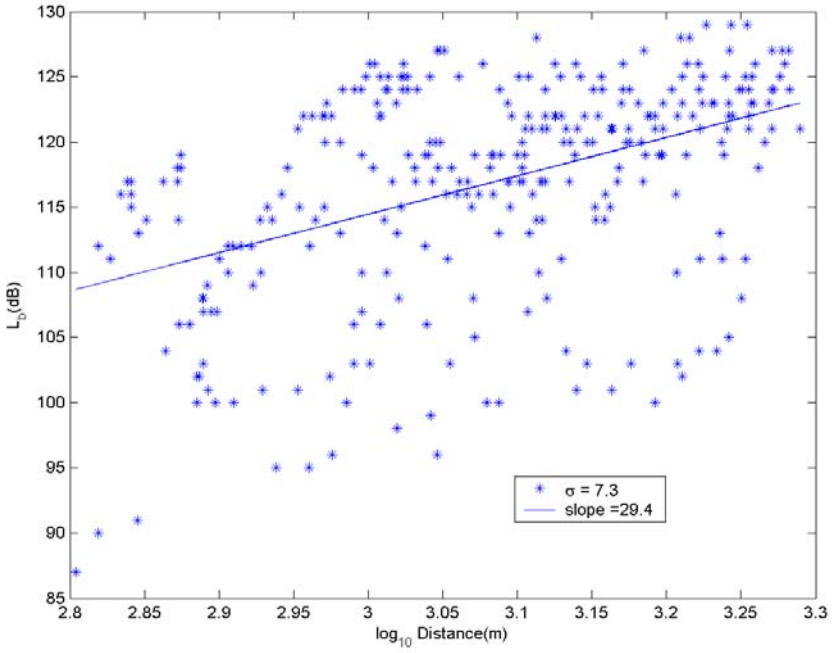

Figure B19. Basic transmission loss versus distance, sector 1 route 2, urban mixed, at 2260 MHz.

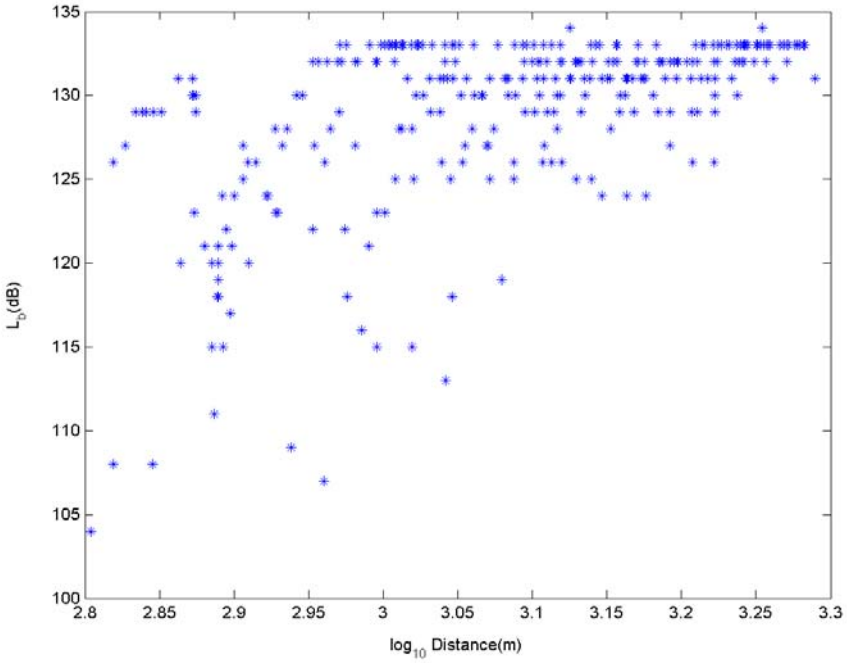

Figure B20. Basic transmission loss versus distance, sector 1 route 2, urban mixed, at 5750 MHz.

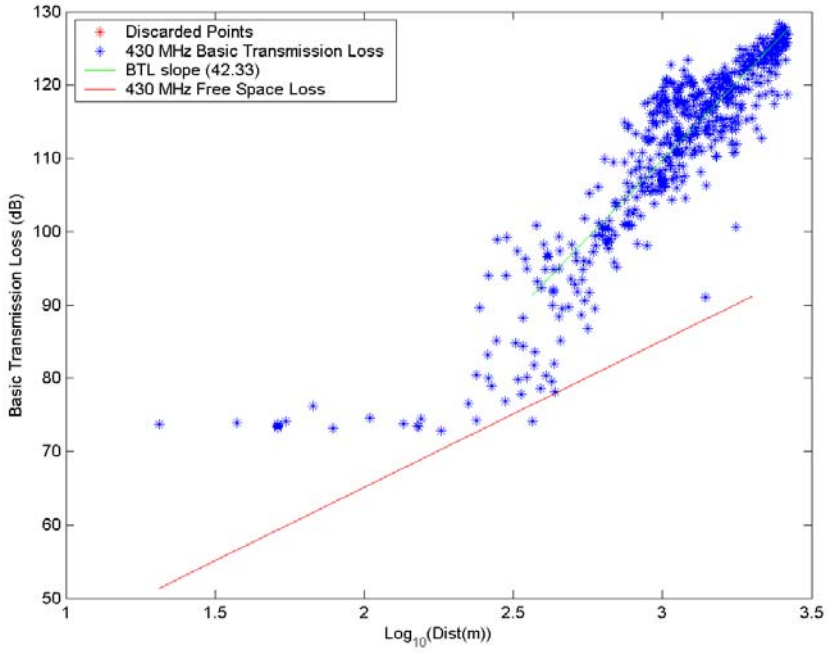

Figure B21. Basic transmission loss versus distance, sector 2 route1, urban high-rise, 430 MHz.

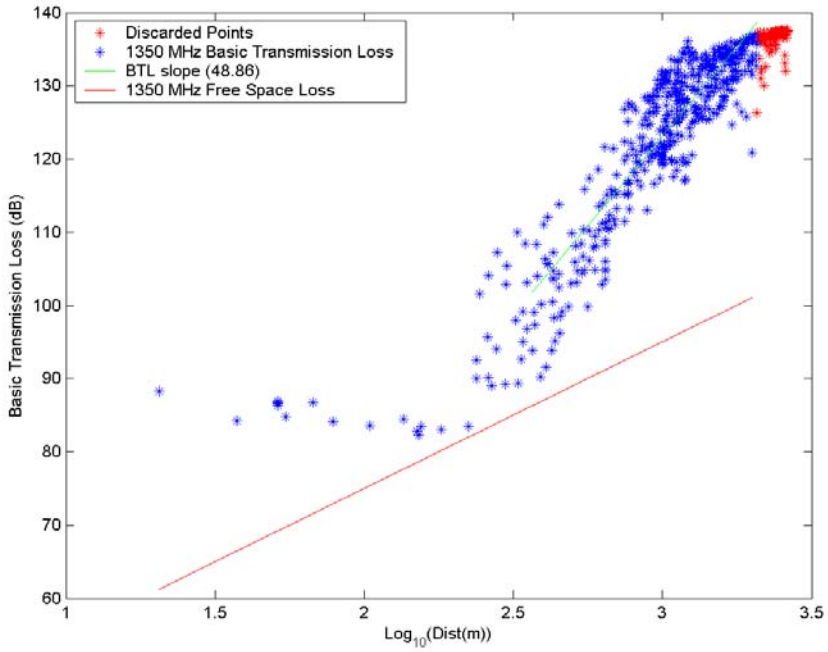

Figure B22. Basic transmission loss versus distance, sector 2 route 1, urban high-rise, 1350 MHz.

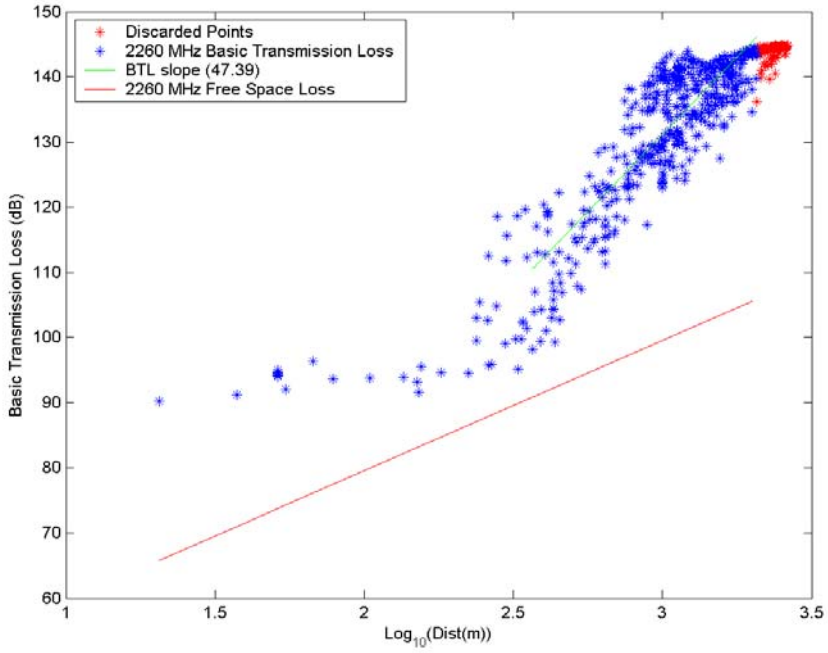

Figure B23. Basic transmission loss versus distance, sector 2 route1, urban high-rise, 2260 MHz.

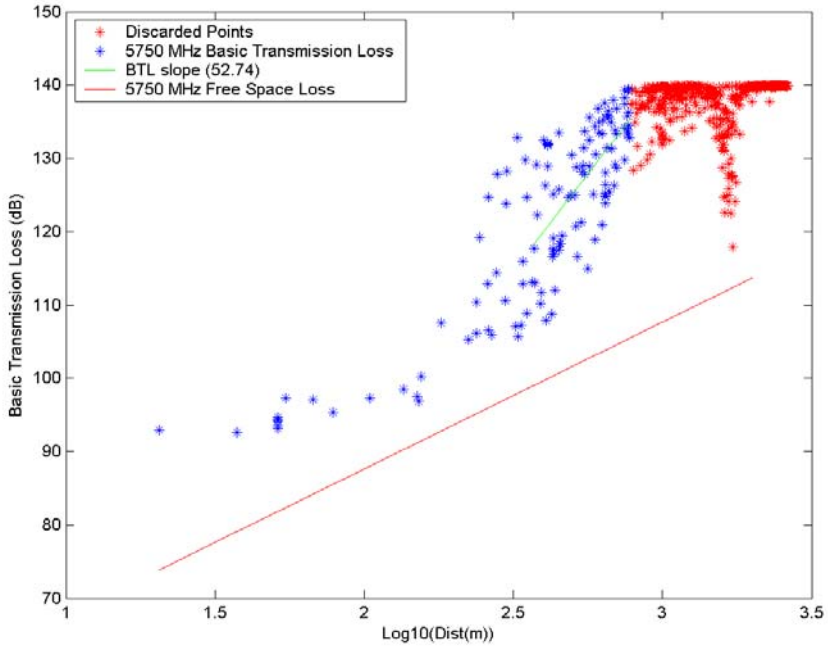

Figure B24. Basic transmission loss versus distance, sector 2 route1, urban high-rise, 5750 MHz.

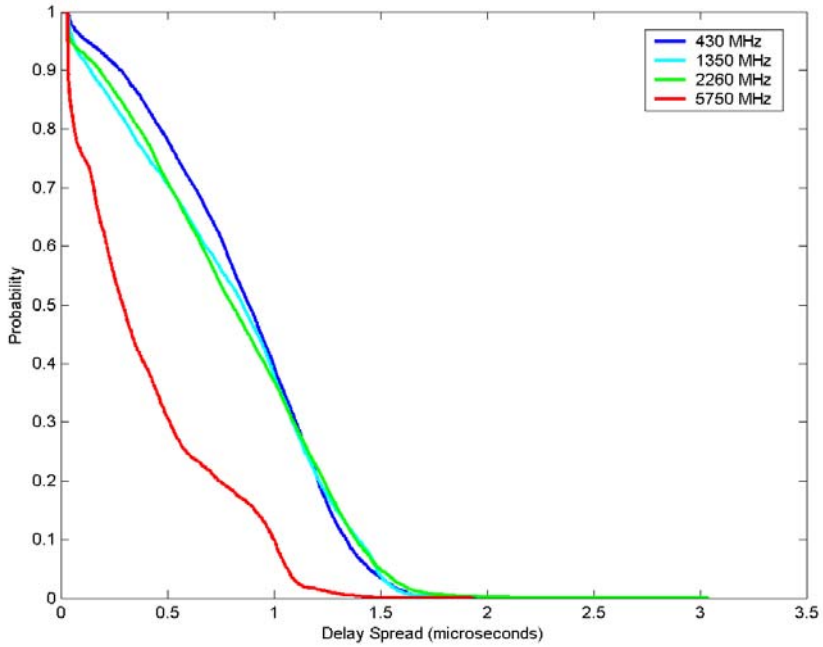

Figure B25. Cumulative distribution of delay spreads, sector 1 route 2, 430-5750 MHz.

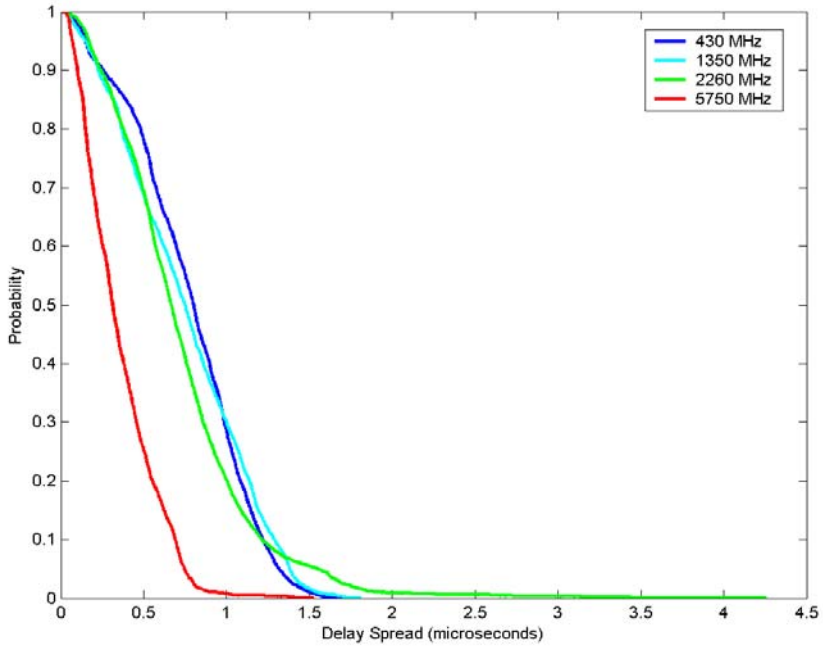

Figure B26. Cumulative distribution of delay spreads, sector 2 route 1, 430-5750 MHz.

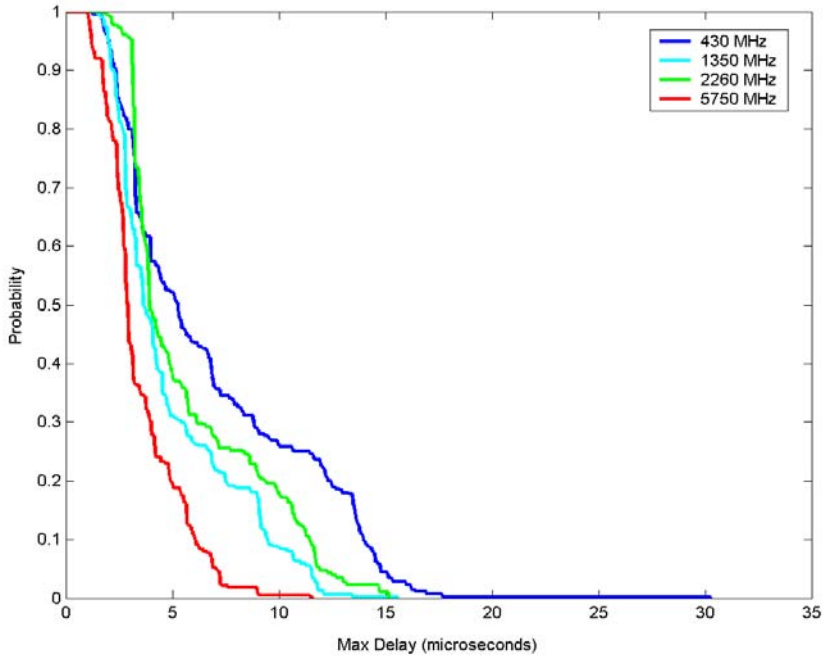

Figure B27. Cumulative distribution of the maximum delay, sector 1 route 1.

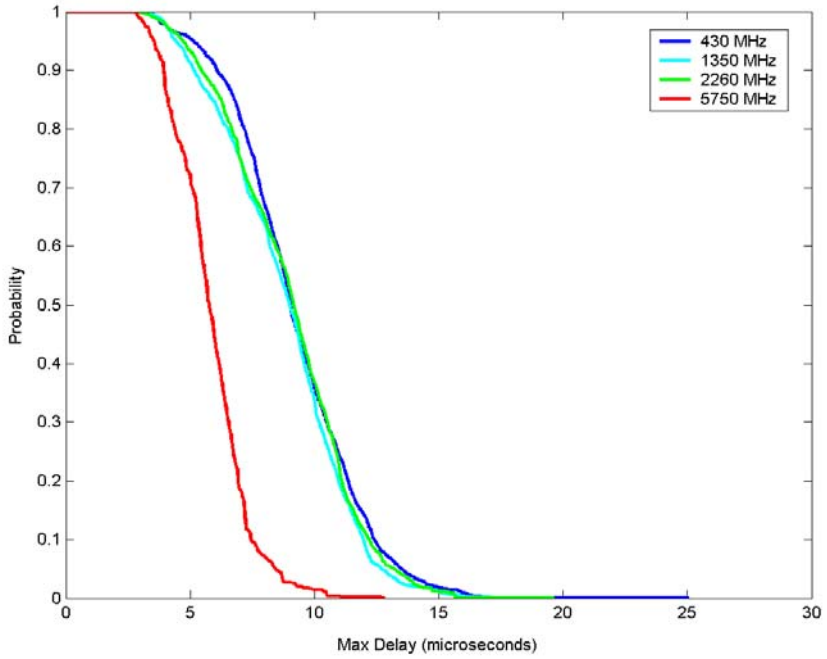

Figure B28. Cumulative distribution of the maximum delay, sector 1 route 2.

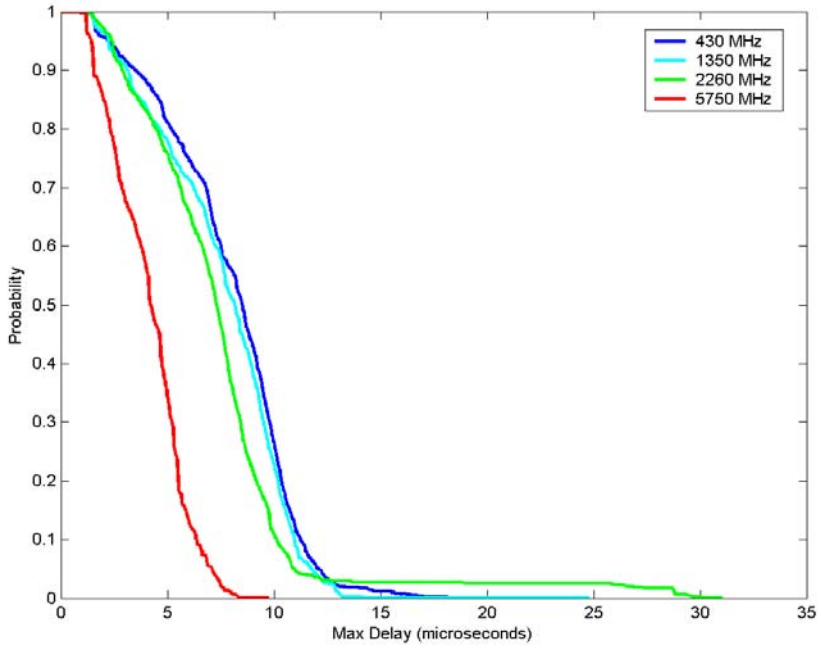

Figure B29. Cumulative distribution of the maximum delay, sector 2 route 1.

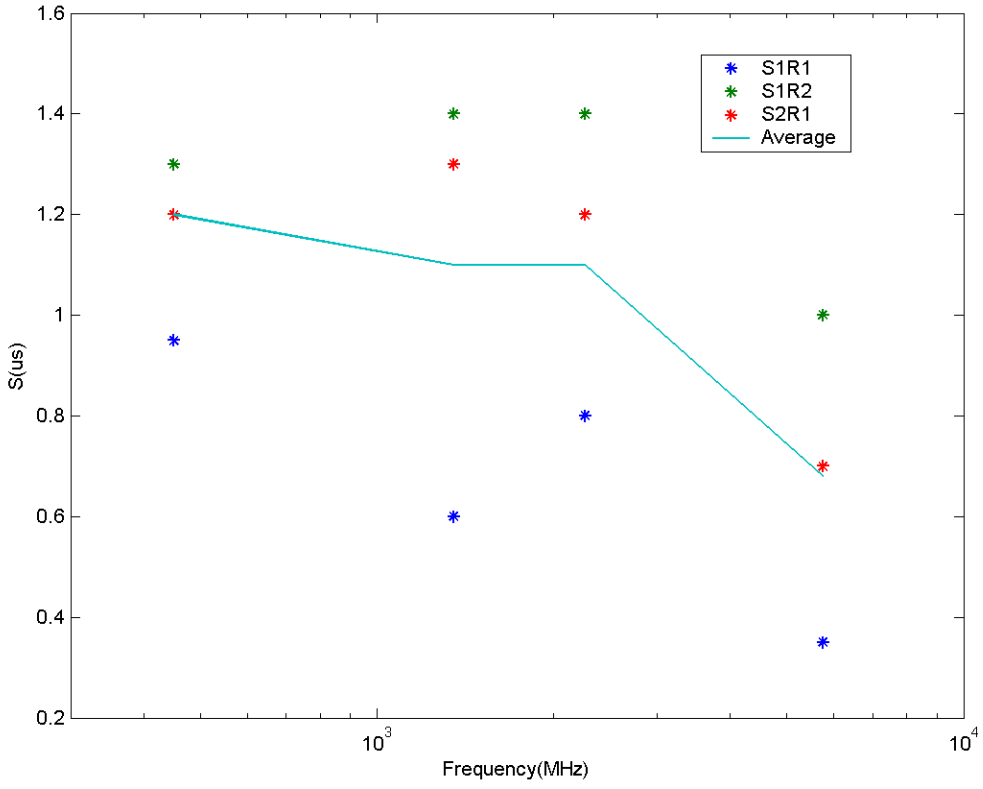

Figure B30. Delay spread not exceeded 90% of the time versus frequency for all drive routes.

FORM **NTIA-29** U.S. DEPARTMENT OF COMMERCE
(4-80) NAT'L. TELECOMMUNICATIONS AND INFORMATION ADMINISTRATION

BIBLIOGRAPHIC DATA SHEET

1. PUBLICATION NO. TR-04-407	2. Government Accession No.	3. Recipient's Accession No.
4. TITLE AND SUBTITLE Relative Propagation Impairments Between 430 MHz and 5750 MHz for Mobile Communication Systems in Urban Environments		5. Publication Date December 2003
		6. Performing Organization Code NTIA/ITS.T
7. AUTHOR(S) Peter Papazian and Michael Cotton		9. Project/Task/Work Unit No. 3108000 300
8. PERFORMING ORGANIZATION NAME AND ADDRESS National Telecommunications & Information Administration Institute for Telecommunication Sciences 325 Broadway Boulder, CO 80305		10. Contract/Grant No.
11. Sponsoring Organization Name and Address NTIA, Herbert C. Hoover Bldg. 14th & Constitution Ave., NW Washington, DC 20230		12. Type of Report and Period Covered

14. SUPPLEMENTARY NOTES

15. ABSTRACT (A 200-word or less factual summary of most significant information. If document includes a significant bibliography or literature survey, mention it here.)

Radiowave propagation measurements made in an urban area of Denver, Colorado, are described. Wideband, impulse response measurements were made at 4 carrier frequencies from 430 MHz to 5750 MHz. These measurements were made using a mobile measurement van to characterize the mobile communications environment. Basic transmission loss and delay spread are characterized by analysis of the path loss slope and delay spread statistics. By analyzing the results versus carrier frequency the relative propagation impairments for communication systems at 430, 1350, 2260 and 5750 MHz are compared. It was found that the path loss slope increased on average by 11 dB/decade and the delay spread decreased from 33% to 65% over the decade of frequencies measured.

16. Key Words (Alphabetical order, separated by semicolons)

basic transmission loss; delay spread; impulse response; path loss; radiowave propagation; urban environment

17. AVAILABILITY STATEMENT UNLIMITED.	18. Security Class. (This report)	20. Number of pages 40
	19. Security Class. (This page)	21. Price:

NTIA FORMAL PUBLICATION SERIES

NTIA MONOGRAPH (MG)

A scholarly, professionally oriented publication dealing with state-of-the-art research or an authoritative treatment of a broad area. Expected to have long-lasting value.

NTIA SPECIAL PUBLICATION (SP)

Conference proceedings, bibliographies, selected speeches, course and instructional materials, directories, and major studies mandated by Congress.

NTIA REPORT (TR)

Important contributions to existing knowledge of less breadth than a monograph, such as results of completed projects and major activities. Subsets of this series include:

NTIA RESTRICTED REPORT (RR)

Contributions that are limited in distribution because of national security classification or Departmental constraints.

NTIA CONTRACTOR REPORT (CR)

Information generated under an NTIA contract or grant, written by the contractor, and considered an important contribution to existing knowledge.

JOINT NTIA/OTHER-AGENCY REPORT (JR)

This report receives both local NTIA and other agency review. Both agencies' logos and report series numbering appear on the cover.

NTIA SOFTWARE & DATA PRODUCTS (SD)

Software such as programs, test data, and sound/video files. This series can be used to transfer technology to U.S. industry.

NTIA HANDBOOK (HB)

Information pertaining to technical procedures, reference and data guides, and formal user's manuals that are expected to be pertinent for a long time.

NTIA TECHNICAL MEMORANDUM (TM)

Technical information typically of less breadth than an NTIA Report. The series includes data, preliminary project results, and information for a specific, limited audience.

For information about NTIA publications, contact the NTIA/ITS Technical Publications Office at 325 Broadway, Boulder, CO, 80305 Tel. (303) 497-3572 or e-mail info@its.bldrdoc.gov.
